MATHEMATICAL MODELING FOR THERMOHYDRAULIC PERFORMANCE OF WIRE MESH PACKED BED SOLAR AIR HEATER

A thesis submitted in partial fulfillment of the requirements for the award of

degree of

MASTER OF ENGINEERING

IN

THERMAL ENGINEERING

Submitted By**:**
AMRITPAL SINGH
Roll No: 801083003

Under the guidance of:

Dr. MADHUP KUMAR MITTAL
Assistant Professor, Deptt. of Mechanical Engg.
Thapar University, Patiala

DEPARTMENT OF MECHANICAL ENGINEERING

THAPAR UNIVERSITY

PATIALA – 147004

JULY, 2012

DECLARATION

I hereby declare that the thesis report entitled **'Mathematical modeling for thermohydraulic performance of wire mesh packed bed solar air heater'** in the partial fulfillment of the requirement of **Master of Engineering in Mechanical (THERMAL) Engineering** to **Thapar University, Patiala,** is a record of candidate's own work carried out by him under the our supervision and guidance. This matter embodied in this report has not been submitted in part or full to any other university or institute for the award of any degree.

Date: 16-07-2012

Place: Patiala

Amritpal Singh

(Amritpal Singh)

This is to certify that above declaration made by the student concerned is correct to the best of my knowledge & belief.

Supervisor

Dr. Madhup Kumar Mittal

Assistant Professor, M.E.D

Thapar University, Patiala.

Countersigned By:

Dr. Ajay Batish

Professor & Head M.E.D

Thapar University, Patiala.

Dr. S. K. Mohapatra

Dean Academics Affairs

Thapar University, Patiala.

ACKNOWLEDGEMENT

With deep sense of gratitude I express my sincere thanks to my guide, ***Dr. Madhup Kumar Mittal*** for his valuable guidance, proper advice and constant encouragement during my thesis work.

I also feel very much obliged to ***Dr. Ajay Batish***, Professor & Head of Mechanical Engineering Department.

I am also very thankful to my friends for their support. Lastly I would like to thank my parents and almighty who deserve gratitude beyond accountability for their valuable blessings.

Amritpal Singh

Roll no: 801083003

ABSTRACT

Solar air heaters are used for low to moderate temperature applications like space heating, crop drying, timber seasoning and other industrial applications. Conventional air heaters are found to have poor thermal efficiency primarily due to low convective heat transfer coefficient between the absorber plate and flowing air, leading to higher plate temperature and greater thermal losses. Attempts have been made to improve the efficiency of solar air heaters by employing various techniques. Use of porous packing's inside the duct is one of the important design improvements to achieve this objective. Packed bed collectors absorb solar radiation in depth which reduces the top layer temperature of the matrix and thus top losses are reduced. Such collectors have high ratio of heat transfer area to volume resulting in high heat transfer capability. Moreover, heat transfer coefficient between packing element and flowing air is also increased due to increased turbulence of flowing air. An attempt to enhance heat transfer is always accompanied with increase in pressure drop and thus pumping power requirement is increased. It is therefore desirable to optimize the system to maximize heat transfer, keeping frictional losses at minimum possible level.

In the present work a methodology has been presented for thermohydraulic optimization of packed bed solar air heater having its flow passage packed with wire screen matrices having various geometrical parameters. The thermohydraulic performance of the system in terms of an effective efficiency is determined on the basis of actual thermal energy gain subtracted by the equivalent thermal energy required to generate power needed for pumping air through the packed bed. A mathematical model is developed to compute effective efficiency, based on energy transfer mechanism in the bed. Based on the results of mathematical model a design criterion has been suggested for selecting a suitable matrix for packing the air flow duct of solar air heater which results in best thermal efficiency with minimum pumping power penalty. The salient results of investigation are as follows:

(i) Solar air heaters packed with wire screen matrix are more efficient than conventional type of air heaters.

(ii) Thermal efficiency as well as effective efficiency of packed bed air heaters depends on the geometrical parameters of the packing element.

(iii) A design criterion has been suggested for selecting the best geometry of matrix resulting in optimum thermohydraulic performance of air heater for given operating conditions.

Table of Contents

LIST OF TABLES:

LIST OF FIGURES:

NOMENCLATURE

A	heat transfer area
A_c	collector plate area, m^2
A_f	frontal area of collector bed, m^2
a_v	heat transfer area per unit volume of bed,
C_c	capital cost of collector, Rs
C_e	capital cost of other equipments, Rs
C_P	specific heat of air, J/kg K
C_p	unit cost of electric power, Rs/kW h
C_u	cost of unitenergy delivered by the solar energy system, Rs/kW h
C_{ml}	annual cost of maintenance with respect to labor, Rs
C_{mm}	annual cost of maintenance with respect to material, Rs
C	conversion factor
C_p	specific heat of air, kJ/(kg K)
d_w	wire diameter of screen, m
D	depth of bed, m
De	equivalent diameter of particle (=6/av),m
Dp	pressure drop in the duct, N/m^2
f_p	friction factor in packed bed
G	air mass flow rate per unit collector area,kg/(s m^2)
G_o	mass velocity of air Kg/s- m^2
h_c	convection heat transfer coefficient between air and matrices, W/(m^2 K)
h_v	volumetric heat transfer coefficient, W/(m^3 K)
I	intensity of solar radiation, W/m^2
I_1	irradiation at the inner surface of lowerglass cover, W/m^2
I_2	irradiation at the bottom plate of packed bed collector, W/m^2
I_y	intensity of solar radiation at depth y from top surface of the bed, W/m^2
J_h	Colburn J-factor (=$StPr^{2/3}$)
K_a	thermal conductivity of air, W/(m K)
Ke	effective thermal conductivity of packedbed, W/(m K)
L	length of collector bed, m
m	mass flow rate of air, kg/s

n	number of screens in a matrix
P	porosity
P_m	Mechanical Power
Pr	Prandtl number
Pt	pitch of wire mesh, m
q_u	useful heat gain, W
Q	volume flow rate, m^3/s
Qr	radiative heat flux at a distance y, W/m^2
rc	reflectivity of glass cover
rh	hydraulic radius (=Pd_w/4 (1 -P)), m
R	radiosity at the top surface of upper glasscover, W/m^2
R1	radiosity at the bottom surface of lowerglass cover, W/m2
R2	radiosity at the bottom plate, W/m2
Ry	radiosity at a distance y from top surface,W/m2
Rep	packed bed Reynolds number (=2GoDe/3(1 _ P)l)
St	Stanton number (=hc/(CpGo))
ta	ambient temperature,^oC
tb	bed temperature, ^oC
tg	air temperature, ^oC
ti	air inlet temperature, ^oC
to	air outlet temperature, ^oC
tp	temperature of packing material, ^oC
Ut	top loss coefficient, $W/(m^2 K)$
V	velocity of air in the duct, m/s
x	distance in horizontal direction from inlet, m
y	distance in vertical direction from top surface, m
β	extinction coefficient, m^{-1}
τ_p	emissivity of back plate
l	dynamic viscosity of fluid, $N s/m^2$
ρ	density of air, kg/m^3
τ	transmissivity of cover glass
$(\tau)_{eff}$	effective transmittance for double glass cover system
η_{eff}	effective efficiency
η_f	efficiency of fan or blower

η_m efficiency of the electric motor used for driving fan

η_{tr} efficiency of electrical transmission from power plant

η_{th} thermal conversion efficiency of power plant

Chapter 1

Introduction

1.1 General

In present's world the prosperity of nation is measured by the energy consumption of that nation, the GDP of country is directly linked with energy consumption. Therefore demand for energy resources is increasing day by day. There are various types of energy resources, but mainly they are divided in to two forms, these are renewable energy resources (solar, air, wind) and nonrenewable energy resources (coal, petroleum). The industrial growth is accelerated by nonrenewable energy resources, but there stock is limited in nature.

The rapid depletion of fossil fuel resources has necessitated an urgent search for alternative energy sources to meet the energy demands for the immediate future and for generations to come. Of many alternatives, solar energy stands out as the brightest long range promise towards meeting the continually increasing demand for energy. The major drawback with this resource is its low intensity, intermittent nature and non availability during night. Even in the hottest region on earth, the solar radiation flux available rarely exceeds 1 kW/m^2. In spite of these limitations, solar energy appears to be the most promising of all the renewable energy resources. Solar energy is contemplated to have a wide range of applications including water heating, air heating, air-conditioning of buildings, solar refrigeration, photo-voltaic cells, green houses, photo-chemical, power generation, solar furnaces and photo-biological conversions to list a few. Out of these, the utilization of solar energy for power generation and heating/cooling of buildings is the subject of active research these days.

Solar air heater is device which is used to increase the temperature of flowing air through the heater. Solar air heaters are used for moderate temperature applications like:

- Space heating.
- Crop drying.
- Timber seasoning.
- Industrial applications.

Conventional air heaters are found to have poor thermal efficiency, primarily due to low convective heat transfer coefficient between the absorber plate and flowing air, leading to higher plate temperature and greater thermal losses. Various attempts have been made to improve the efficiency of solar air heaters by employing different designs and flow arrangements such as porous packing and artificial roughness.

Use of porous packing inside the solar air heater duct is one of the important design improvements that have been proposed to achieve the objective of improved thermal performance. The major reason of interest in porous packing include high heat transfer area density resulting in high heat transfer capability; energy absorption in depth, resulting in the reduction of the top layer temperature of porous matrix and energy loss from top of the collector is reduced and increased turbulence of the flowing air resulting in enhanced heat transfer coefficient. Further they can be fabricated with a little additional expenditure over the conventional air heaters. In view of the above, air heaters with porous packing inside its flow duct is a suitable choice for improving the thermal performance of conventional solar air heaters.

A review of the heat transfer studies in packed beds indicate that sufficient research work has been carried out on packed beds used for applications in chemical reactor, compact heat exchangers and heat storage equipment. Even sufficient work has been done in the area of pack bed solar heaters using various types of packing materials and geometries for enhancement of thermal performance. Use of wire screens to form a matrix inside the solar air heater duct is one of the simple, economical and convenient methods.

1.2 OBJECTIVES OF THE PRESENT WORK

1 To investigate the effect of Reynolds number and mass low rate on effective efficiency of different types of matrices.
2. To develop the mathematical models to predict the effective efficiency, pumping power and temperature rise parameter for solar air heater with various matrices.
3. To investigate the effect of temperature rise parameter on effective efficiency with packing and without packing.

1.3 ORGANISATION OF THESIS

In this thesis report optimization of wire mesh packed solar air heater is presented. On the basis of mathematical model simulation results are explored.

Chapter 1

This chapter describes general introduction of solar air heater and objective of work.

Chapter 2

It includes review of literature of various experimental and theoretical works by various persons using different techniques to improve performance of solar air heater.

Chapter 3

This section is related with development of mathematical modeling to predict performance characteristics of packed bed solar air heater.

Chapter 4

In it results are obtained and plotted which depicts variation of energy gain and pumping power with respect to mass flow rate, Reynaldo's number and temperature rise parameter.

Chapter 5

In this section conclusion of simulation is drawn.

Chapter 2

Review of literature

In this chapter, an extensive review of literature in the area of solar energy collection system, with special reference to packed bed solar air heaters, is being presented. It has been brought out that there are several schemes that can be implemented to enhance the thermal performance of this most commonly employed energy collection devices. These methods, along with their enhancement potential have been discussed in this chapter.

2.1 Solar Collectors

This equipment absorbs the incoming solar radiant energy converting it into thermal energy at the absorbing surface and transferring this energy to a fluid flowing through the collector. There are two types of solar collectors namely the flat plate and the concentrating collector. A flat plate collector has the area of interception same as that of absorption for solar radiations while a concentrating collector usually has concave reflecting surface to intercept and focus the sun's beam radiation on to a smaller receiving area, thereby increasing the radiation flux substantially.

2.1.1 Flat Plate Collectors

A flat plate collector basically consists of a flat surface with high absorptivity for solar radiations, called the absorbing surface; typically a metal plate, painted black. The energy is transferred from the absorber plate to a carrier fluid circulating across the collector. Thermal

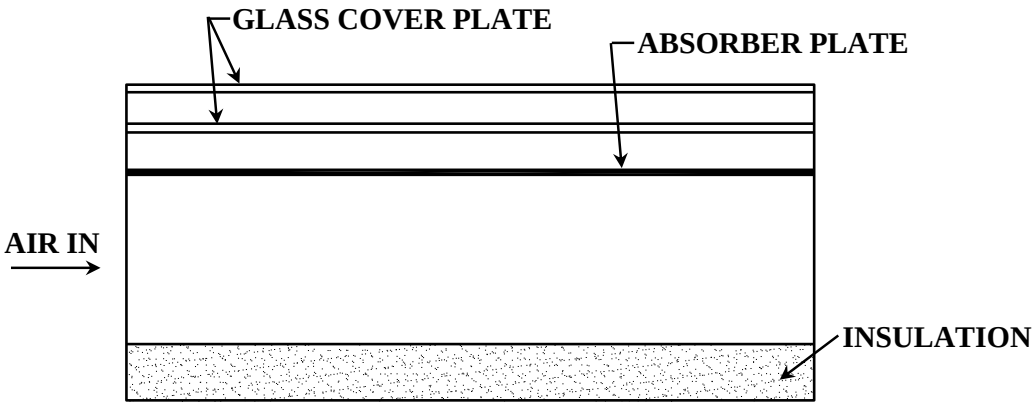

Fig: 2.1.Schematic of smooth flat plate collector (Choudhury *et al* 1993).

insulation is usually placed on the rear side to prevent heat losses. The front side has transparent covers, generally glass that allows transmission of incoming solar radiations but is opaque to the infrared radiations form the absorber plate. Flat plate collectors are usually permanently fixed in position and require no tracking of the sun. The collector should be oriented directly towards the equator, facing south in the northern hemisphere and facing north in the southern hemisphere. For year round applications, the optimum tilt angle of collector is equal to the latitude, whereas for winter, tilt angle should be approximately 10° to 15° more than the latitude and for summer, tilt angle should be approximately 10° to 15° less than latitude. Temperature upto a maximum of about 100 °C above ambient can be achieved through flat plate collectors. Flat plate solar collectors may be divided into two main classifications based on the type of heat transfer fluid used i.e. liquid heating and air heating collectors.

2.1.1.1 Liquid heating collectors

A liquid heating collector comprising a glass covered metal box containing an absorber plate to which an array of tubes is attached and has thermal insulation beneath. Liquid from a storage tank passes through these tubes, picks up heat from the absorber plate and then returns to the storage tank. The flow may be thermosyphonic or forced. The effective collector area of most commercially available collectors ranges from 1 to 2 m^2 with the length being usually larger than the width.

2.1.1.2 Air heating collectors

Flat plate air heating collectors, because of their inherent simplicity, are cheap and most widely used collection device. These have found several applications including space heating and crop drying. A typical configuration of flat plate air heating solar collector is shown in Figure. 2.1. A conventional solar air heating system generally consists of an absorber plate with another parallel plate below it forming a passage for air with a high width to depth ratio. The solar radiations pass through the transparent cover or covers and impinge on the blackened absorber plate and then are transferred to the air flowing beneath the absorber plate.

2.1.2 Concentrating Collectors

Energy flux density on the receiver surface is considerably increased by concentrating collectors which are used for high temperature applications. Concentrating collectors use only beam solar radiation. Such collectors have lower thermal losses but considerably high optical losses. Besides this concentrating collector most of them continuously track the sun.

2.2 Classification of Solar Air Heaters

Solar air heaters can be classified as:

(a) Air heaters with non porous absorbers

(b) Air heaters with porous absorbers

2.2.1 Air Heaters with Non Porous Absorbers

Air heaters with non porous absorbers are those in which air flows above and/or behind the absorber plate as shown in Figure. 2.1. In the conventional design, air flows behind the absorbing surface. There is another design of heater where air flows between the cover glass and the absorber plate. Air heaters of this type are simpler in design but yield lower efficiencies because of increased convective losses from cover glass. There is another arrangement in which air flows between the cover glass and absorber plate and also through the passage below the absorber plate.

2.2.2 Air Heaters with Porous Absorbers

In this type of air heaters, incoming radiations are absorbed as these travel through a porous bed consisting of packing elements of different shapes, sizes and porosities. Various types of packing elements used for solar air heaters include metal sphere, glass beads, crushed glass, iron turnings, slit and expanded aluminum foils and wire screens. Figure 2.2 illustrates basic design feature of these solar air heaters. Porous absorbers offer several advantages which include high heat transfer area to volume ratio, high heat transfer coefficient and absorption of energy ‘in depth’ resulting in reduced top layer temperature and thus less heat losses with higher efficiency.

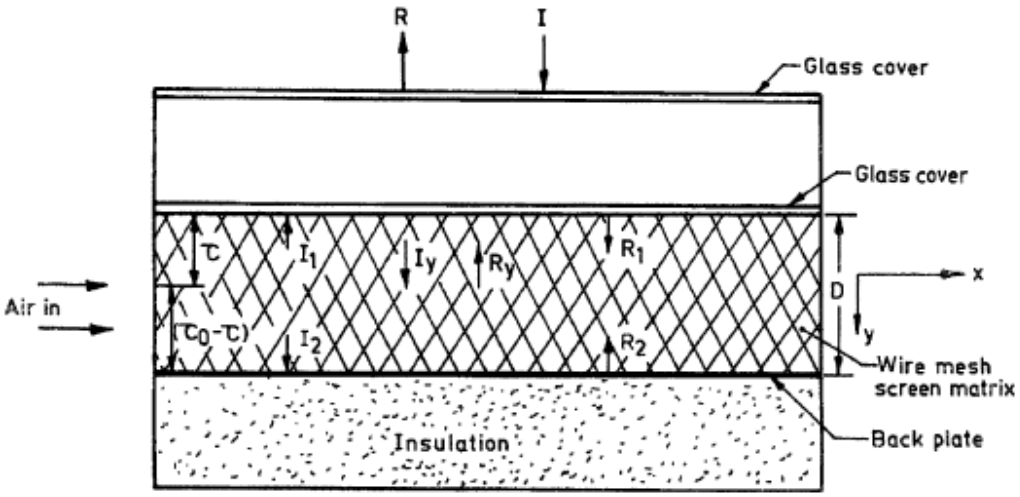

Fig 2.2: Schematic of packed bed solar air heater (Choudhury *et al* 1993).

2.3 Thermal Performance of a Flat Plate Solar Collector

Performance of a flat plate collector was first investigated by Hottel and Woertz (1942). It is assumed that the rate of useful heat collection is equal to the rate at which solar energy is being absorbed minus the heat loss rate. They proposed relationship for determining the rate of useful thermal energy collection of a flat plate collector, q_u, operating under quasi-steady state conditions as follows:

$$q_u = I(\tau\alpha) - U_L(\bar{t}_p - t_a) \tag{2.1}$$

Where, I is the intensity of solar radiation

U_L is the overall heat loss coefficient

$\bar{t}_p$ is the mean plate temperature

t_a is the ambient temperature

The term $(\tau\alpha)$ represents transmittance absorbance product, which accounts for the complex interaction of optical properties of the glass cover and absorber plate. In fact, the average absorber plate temperature $\bar{t}_p$ depends upon geometry of collector, incident solar radiations, fluid flow rate and the properties of collector fluid. Bliss (1959) proposed an alternative equation

incorporating a new parameter F′, known as collector efficiency factor in terms of average fluid temperature $\bar{t}_f$ as follows:

$$q_u = F'[I(\tau\alpha) - U_L(\bar{t}_f - t_a)] \tag{2.2}$$

Bliss (1959) also modified Eq. (2.1) to a still more practically usable form as below:

$$q_u = F_R[I(\tau\alpha) - U_L(t_i - t_a)] \tag{2.3}$$

Where F_R is termed as collector heat removal factor. Hottel and Whillier (1955) obtained an expression for heat removal factor, F_R, as follows:

$$F_R = (G\,C_p / U_L)\left[1 - \exp(-F'\,U_L / G\,C_p)\right] \tag{2.4}$$

Solar collector efficiency η has been expressed as:

$$\eta = \frac{q_u}{I} \tag{2.5}$$

From Eqs. (2.1), (2.2), (2.3) and (2.5), the following relationships are obtained:

$$\eta = \left[(\tau\alpha) - U_L\left(\frac{\bar{t}_p - t_a}{I}\right)\right] \tag{2.6}$$

$$\eta = F'\left[(\tau\alpha) - U_L\left(\frac{\bar{t}_f - t_a}{I}\right)\right] \tag{2.7}$$

$$\eta = F_R\left[(\tau\alpha) - U_L\left(\frac{t_i - t_a}{I}\right)\right] \tag{2.8}$$

Eqs. (2.6), (2.7) and (2.8) are known as Hottel -Whillier and Bliss equations. These equations are widely used for comparing thermal performance of collectors and also to determine the effect of the changes in system and operating parameters on the collector efficiency.

Biondi *et al.* (1988) have proposed following equations for efficiency of solar heater drawing ambient air:

$$\eta = F_o\left[(\tau\alpha) - U_L\left(\frac{t_o - t_i}{I}\right)\right] \tag{2.9}$$

Where F_o is the heat removal factor referred to outlet air temperature and is expressed as :

$$F_o = \frac{GC_p}{U_L}\left[\exp\left(\frac{U_L F'}{GC_p}\right) - 1\right] \tag{2.10}$$

2.3.1 Overall Heat Loss Coefficient, U_L

An accurate determination of heat loss coefficient, U_L, is important for the determination of solar collector efficiency, as can be noted from Eqs. (2.6) to (2.9). It is known that the overall loss coefficient is the sum of its component, namely: top, bottom and edge loss coefficients U_t, U_b and U_e, as written below:

$$U_L = U_t + U_b + U_e \tag{2.11}$$

2.3.1.1 Top loss coefficient, U_t

Hottel and Woertz (1942) developed a semi-empirical relationship for top loss coefficient, U_t, which is as given below:

$$U_t = \left[\frac{N}{C\left[(\overline{T}_p - T_a)/(N + f_t)\right]^{0.25}} + \frac{1}{h_w}\right]^{-1} + \frac{\sigma\left(\overline{T}_p^2 + T_a^2\right)\left(\overline{T}_p + T_a\right)}{1/\varepsilon_p + \left[(2N + f_t - 1)/\varepsilon_c\right] - N} \tag{2.12}$$

Klein (1975) recommended an empirical correlation for the top loss coefficient for a range of absorber plate temperature up to 200 °C. This correlation predicts top loss coefficient, U_t within ± 0.3 W/m^{2}K and is given by:

$$U_t = \left[\frac{N}{\left(C / \overline{T}_p\right)\left[\left(\overline{T}_p - T_a\right)/(N + f_t)\right]^e} + \frac{1}{h_w} \right]^{-1}$$

$$+ \frac{\sigma\left(\overline{T}_p^2 + T_a^2\right)\left(\overline{T}_p + T_a\right)}{(\varepsilon_p + 0.00591\ N\, h_w)^{-1} + [(2N + f_t - 1 + 0.133\varepsilon_p)/\varepsilon_p] - N} \qquad (2.13)$$

Where,

f_t = $(1+0.089\ h_w - 0.1166\ h_w\ \varepsilon_p)\ (1+0.07866\ N)$

e = $0.43\ (1-100/t_p)$

C = $520\ (1-0.000051\ s^2)$ for $0° \le s \le 70°$

For $70 \le s \le 90$, use $s = 70°$

A similar equation for top loss coefficient, U_t was suggested by Agarwal and Larson (1981) which yields the value of top loss coefficient within ± 0.25 W/m^2 °C as:

$$U_t = \left[\frac{N}{\left(\frac{C}{T_p}\right)\left(\frac{\overline{T}_p - T_a}{N + f_t}\right)^{0.33}} + \frac{1}{h_w} \right]^{-1} + \frac{\sigma\left(\overline{T}_p + T_a\right)\left(\overline{T}_p^2 + T_a^2\right)}{\left[\varepsilon_p + 0.05N(1 - \varepsilon_c)\right]^{-1} + \left[\frac{2N + f_t - 1}{\varepsilon_c}\right] - N} \qquad (2.14)$$

Where,

f_t = $(1-0.04\ h_w + 0.005\ h_w^2)\ (1+0.091\ N)$

C = $250\ [1-0.0044\ (s-90)]$

In order to consider the effect of tilt angle and the gap spacing, Malhotra *et al.* (1981) have proposed following correlation:

$$U_t = \left[\frac{N}{\left(204.3/\overline{T}_p\right)\left[L_s^3 \cos s\left(\overline{T}_p - T_a\right)/\left(N + f_t\right)\right]^{0.252} L_s^{-1}} + \frac{1}{h_w} \right]^{-1}$$

$$+ \frac{\sigma\left(\overline{T}_p + T_a\right)\left(\overline{T}_p^2 + T_a^2\right)}{\left[\varepsilon_p + 0.0425\, N(1-\varepsilon_{p)}\right]^{-1} + \left[\frac{2N + f_t - 1}{\varepsilon_c}\right] - N} \qquad (2.15)$$

Where,

f_t = $(9/h_w - 30/h_w^2)\,(T_a/316.9)\,(1+0.91\,N)$ and

Mullick and Samdarshi (1988) have obtained an equation for U_t as given below:

$$U_t = \left[\left\{ \frac{12.75\left((\overline{T}_p - T_c)\cos s\right)^{0.264}}{\left(\overline{T}_p + T_c\right)^{0.46} L_s^{0.21}} + \frac{\sigma\left(\overline{T}_p^2 + T_c^2\right)\left(\overline{T}_p + T_c\right)}{1/\varepsilon_p + 1/\varepsilon_c - 1} \right\}^{-1} \right.$$

$$\left. + \left\{ h_w + \frac{\sigma\varepsilon_c\left(T_c^4 - T_s^4\right)}{(T_c - T_a)} \right\}^{-1} + \frac{d_c}{k_c} \right]^{-1} \qquad (2.16)$$

2.3.1.2 Bottom loss coefficient, U_b

Considering the conductive heat transfer through insulation and convective heat transfer from bottom of the collector to environment, bottom loss coefficient is calculated as follows:

$$U_b = \left[\frac{\delta}{k_{ins}} + \frac{1}{h_b} \right]^{-1} \qquad (2.17)$$

2.4 Performance Enhancement Techniques for Solar Air Heaters

The performance of a flat plate solar air collector has been found to depend strongly on the rate of incident solar radiations, the losses from the absorber surface and the rate of heat transfer from absorber plate to the air. The following are some performance enhancement techniques for solar air heater.

2.4.1 Reduction of Thermal Losses

The following are some of the design modifications used for the enhancement of thermal efficiency of collectors, by reducing thermal losses.

2.4.1.1 By using alternate medium or vacuum in the gap space

Convective heat losses can be minimized by optimizing the gap space and the use of alternate medium in the space between two covers. Malhotra *et al.* (1980) have shown that the use of heavy gases can reduce the heat losses by 34%. Alternatively, partial evacuated space by 10% reduction in pressure can reduce losses by 85%. It has also been shown that a combination of moderate vacuum and a selective surface (α_s = 0.9; $\in_s$ = 0.15) can increase the daily energy collection by as much as 27.8% and can make it possible to operate the collector at 150 °C with a daily energy collection efficiency of more than 40%.

2.4.1.2 By using selective absorber surfaces

Selective surfaces are especially important when the collector plate temperature is much higher than the ambient air temperature, and usually the largest heat losses are through emittance from the collector surface. The maximum radiation loss appears at the wave length of about 10 microns if the collector plate is close to room temperature and at about 5 microns if collector plate temperature is around 300 °C. If the absorbing surface of the collector is treated such that it absorbs most of the solar energy between 0.3 micron and 2.5 microns and it emits only a small fraction of the infrared radiation, it is possible to increase the efficiency of solar energy collector significantly.

2.4.1.3 By using multi pass system

The thermal losses from the glass cover of the single, two or more glass cover air heater can be reduced by using a two pass system. In a two pass solar air heaters, the air flows first through the space between glass cover and absorber plate and then through the normal duct. The concept of two pass air heater was introduced by Satcunanathan and Deonarine (1973). They concluded that the two pass design had an efficiency which was about 10-15 percent higher than the single pass design. It has been reported that outer glass temperature was lower by 2–5 °C over the day and were much nearer to the atmospheric temperatures compared to those when collector was operated in a conventional single pass mode.

Wijeysundera *et al.* (1982) developed heat transfer models for two pass flow arrangement and compared the results of these models with that of single pass system. It was found from the study that for open systems, with inlet air at ambient temperature, the two pass systems gave efficiency about 10-15 percent more than that of the single pass system over a wide range of design and operating conditions.

Togrul and Pehlivan (2004) had investigated the effect of selective absorbing surface (stainless steel painted with black absorber paint) and packing in the two-pass airflow passage of the absorbing tube on efficiencies of a solar air heater with a conical concentrator. As a packing material they used aluminum wire mesh with a variety of folding Beside these, various aspects of the heat and fluid flow in the absorbing tube as influencing the system performance were observed by evaluating friction factors, pumping power, convective heat transfer coefficients and Colburn factors for empty and packed airflow passage of the absorbing tube. It was observed that using absorber with selective surface reduces heat loss to ambient. Furthermore efficiency can be increased by placing pacing inside the flow channel. Outlet temperature of air is increasing with the increase in folds. They compared selective absorbing surface and pacing air heater with air heater without them, there is difference of 30% in efficiency of these two air heaters. The main reason behind it is reduction in heat transfer coefficient of these two heaters. It was observed with decrease in heat transfer coefficient rise in temperature of air increases. In this system problem of changing face of collector with respect to sun is occurred.

Naphon (2005) carried research on effect of porous media on the performance of double pass flat plate solar air heater. The mathematical model was developed which describes heat transfer

characteristics derived from energy conversion equations for double pass air heater. The mathematical model was solved by finite difference method using implicit technique. The results obtained from the model are validated by comparing with experimental data of previous researchers. The result with porous media shows the efficiency of solar air heater is 25.9% higher than the thermal efficiency of solar heater without porous media.

2.4.1.4 By using selective coatings and double pass system

Dhiman *et al* (2011**)** had studied "Parallel flow Packed bed solar air heater "in which the air is passed simultaneously and separately over and under the absorber plate as shown in Figure 2.3 it was double channel design with double air flow between cover and absorber plate and between absorber and back plate it was designed to reduce front cover losses of collector. The mild steel machining chips are used to pack the bed. The machining chips were kept in upper duct above the absorber plate to enhance thermal performance. They developed mathematical model and compared the results of mathematical model with the experimental. In mathematical model mass flow rate and porosity are variable parameter. The result of mathematical model show that thermal efficiency increases as the mass flow rate increases or porosity decreases.

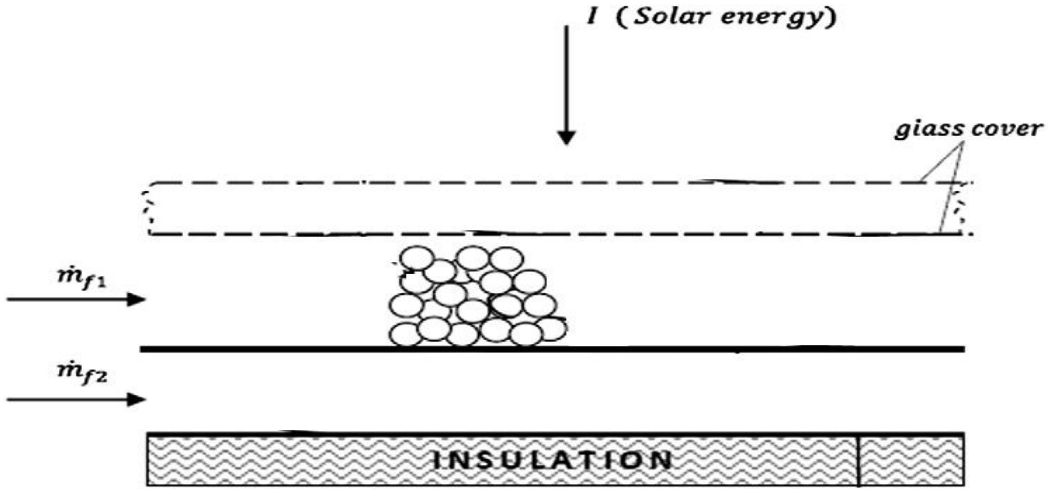

Fig.2.3. Schematic diagram of parallel flow packed bed solar air heater (Dhiman et al 2011)

2.4.1.5 By using obstacles and selective coating

Akpinar and Kocyigit (2010) experimentally carried out performance of solar air heater using three different types of obstacles and without obstacles. They performed it on two mass flow rates. In their design they divide absorber plate with rectangular obstacles and absorber was made of stainless steel with black chrome as selective coating. The experiment is performed with triangular obstacles, leaf shaped obstacles (5X5cm) with 10cm intervals and rectangular obstcale

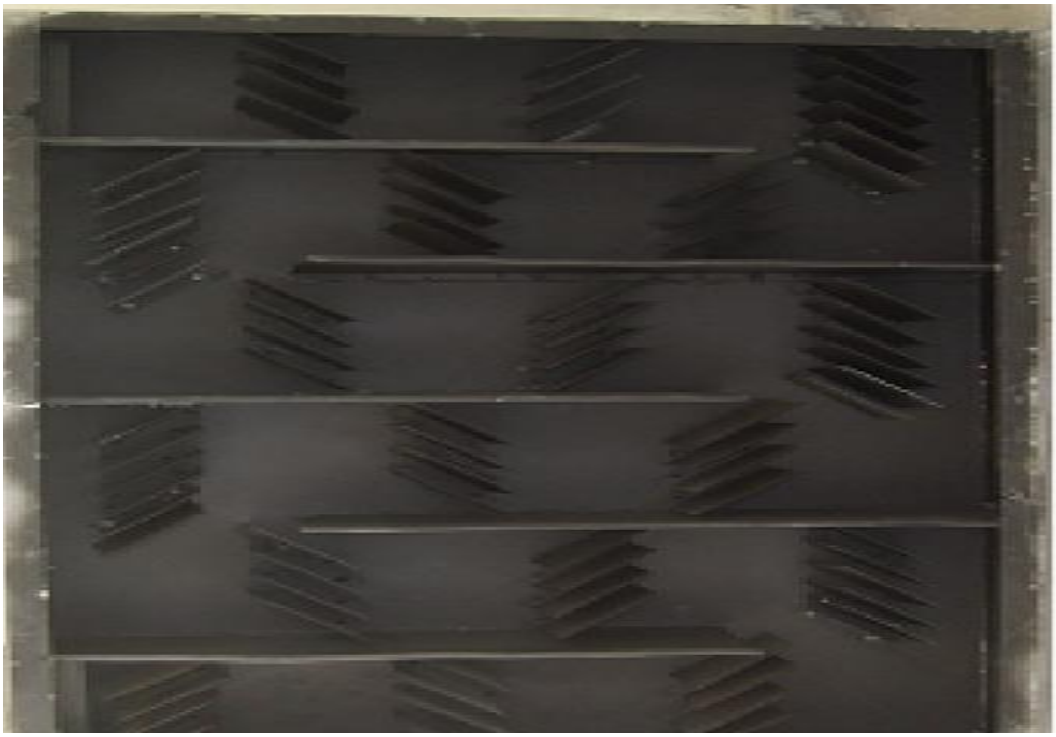

Fig.2.4.Rectangular obstacles inclined at 45^0 (Akpinar and Kocyigit 2010)

(10X10) with 2.5cm intervals with inclination of 45^0 as shown in Figure 2.4 and without any obstacle in solar air heater.Further energy analysis and exergy analysis are done. Under energy analysis unsteady state is considered where as in exergy analysis steady state, steady flow, negligible effect of kinetic energy and potential energy on chemical or nuclear reactions and air acts as an ideal gas. It was observed while using these models, highest temperature rise occurs at afternoon. The maximum temperature difference occurs with leaf shaped obstacle followed by rectangular, triangular obstacle and without obstacle because of turbulence, although the pattern for thermal efficiency is different because it depends upon temperature rise and area of collector.

Thermal efficiency is higher for leaf shaped obstacle followed by without obstacle, triangular and rectangular obstacle. There was decrease in efficiency as temperature parameter $(T_{out} - T_{in})/I$ increases, because the overall loss was lower at higher temperature parameter.

2.4.1.6 By using multi pass and obstacles

Ozgen *et al* (2009) had performed experimental study of thermal performance of double flow solar air heater with aluminum cans as shown in Figure 2.5. It was observed that performance of double flow solar air heater is more efficient than that of single flow channel due to increase in heat transfer area which is double in case of double flow solar air heater as compared with single flow channel. Test results shows that higher efficiency is for non arranged cans than that for without cans. The reason behind the higher efficiency with can compared to without is, obstacle create turbulence and reduces dead zone in the collector.

Fig 2.5 Absorber plate used in collector with obstacles (Ozgen *et al* 2009)

2.4.1.7 By using multi pass, selective coating and obstacles

Esen (2007) carried experimental study of energy and exergy analysis of double flow solar air heater having different obstacles on absorber plate as shown in Figure 2.6 The absorbers were constructed from stainless steel with selective coating of black chrome. It was crystal clear from the results for solar air heater using difent type of obstacles that the introduction of obstacle is

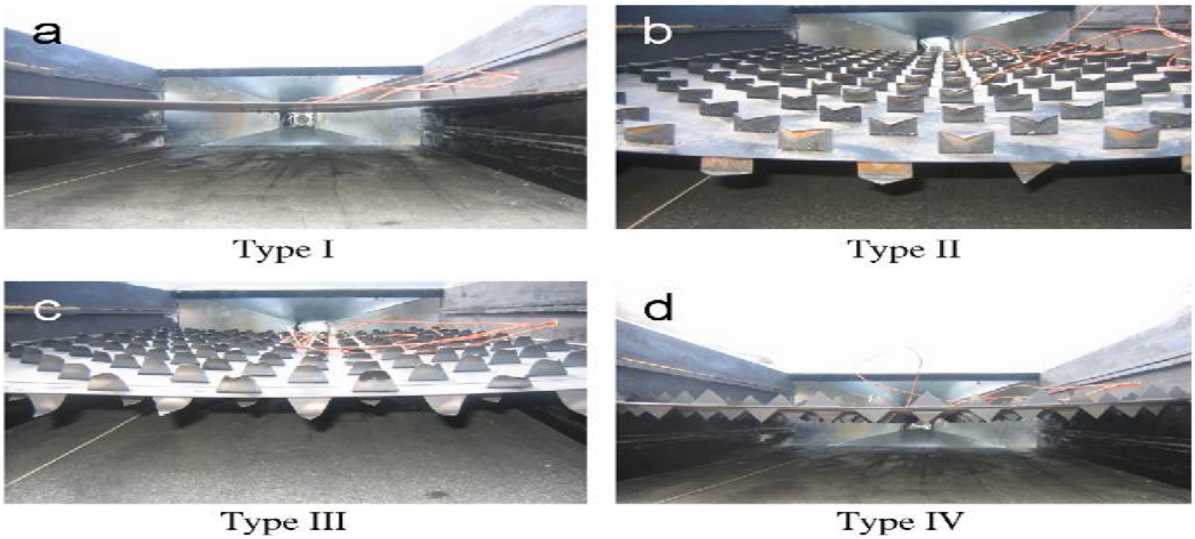

Fig: 2.6 Absorber plate used in collector various obstacles (Esen 2007)

very important for the collector efficiency , although it was observed that the form, dimensions, orientation, and disposition of the obstacles considerably influence the collector efficiency. It was observed that the largest irreversibility occur at flat plate solar air heater without any obstacle.

2.4.1.8 By using thermal energy storage material

Ozturk and Bascetincelik (2003) used volcanic material in solar air heater duct to store solar energy as sensible thermal energy as shown in Figure 2.7; Further this energy is used in green house in fields. The main objective of the study was to determine efficiency of daily storage in a packed bed storage unit and also to compare energy efficiency of the packed-bed heat storage unit with its exergy efficiency. The feasibility of using heat storage material as a possible alternative to other storage techniques was also considered in this study. Exergy analysis is helpful to determine the reasons for the thermodynamic faults of the thermal and chemical processes. Exergy analysis is also helpful in cost effective design and management of complex processes.

Irigollen *et al* (2003) had purposed and validated a mathematical model describes the dynamics of the heat transfer in an inflatable tunnel solar collector for air heating. In it thermal inertia of pebble bed acting as absorber surface is considered. In mathematical model, the dimensionless version of equation was converted into liner conical form of first order and solved by discretization of equation in an explicit form. For validation of mathematical program was run under the realistic and boundary conditions. The causes for deviation in temperature of experimental and mathematical models was due to under estimation of convective heat transfer coefficient of the pebbles to the fluid, over estimation of absorber thermal capacitance which causes a slight phase shift of theoretical temperature curve relative to experimental curve. Small deviation shows model closely relates with experimental one.

Jain (2006) had developed a mathematical model for reversed absorber plate with natural air flow. This model computes air temperature and various functional component of drying system. In parametric study the effect of width of airflow channel and height of packed bed on the crop temperature was studied. While using reversed absorber plate thermal losses from the collector plate were reduced. In this system flow of air was maintained by thermal buoyancy by absorbing

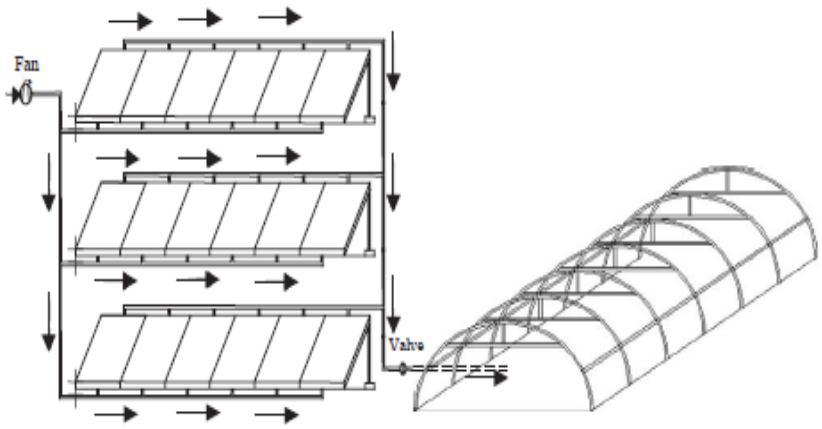

Fig: 2.7 The arrangement of heat storage (Ozturk and Bascetincelik 2003)

energy from upper inclined absorber plate, while absorber plate at bottom supplies heat to incoming air, which further heats pebble, crops in trays simultaneously. Packed bed discharge the energy, which was stored during the off sunshine hours. In this system flow of air is around the clock because of thermal energy storage. Highest temperature is obtained with width at 0.04m and lowest at 0.2m.

Mohamed Rady (2009) had used multiple granular phase change composites with different phase changes in packed bed thermal energy storage system. In this study two or more granular phase change composites (GPCC) are used. Then a mathematical model was developed for analysis of charging and discharging process dynamics at different values of mixing ratios and Reynolds number. In this study two GPCCs (Rubitherm GR27 and GR41) were employed in a packed bed storage system. Due to low phase change temperature range of the two GPCCs (21–29 ^{0}C for GR27 and 31–45 ^{0}C for GR41. It had been observed that rather using single GPCC mixture of GPCCs in a composite bed can result in enhancement overall storage of unit. The optimum mixture strength of GR27 and GR41 is also compared with equal mixture strength. Optimum range is calculated using exergy analysis.

2.4.1.9 By using honeycomb structures

This involves inclusion of a honeycomb panel placed between absorber plate and the cover. The honeycomb of different geometric shapes such as square cells and rectangular cells has been employed. A properly designed cell structure placed between the solar absorber and outer cover glass can substantially reduce natural convection and infrared radiation heat losses. Glass has merit for such cellular structure and it is inexpensive, abundant and has low thermal conductivity which reduces heat losses due to conduction through the walls of the honeycomb material.

2.4.2 Improvement of Heat Transfer from Absorber Plate

The low heat transfer rate from absorber plate to air in the duct results in relatively higher absorber plate temperature leading to higher thermal losses to the environment. These losses can be reduced by lowering the absorber plate temperature by increasing the heat transfer coefficient between absorber and air. This can be achieved by way of following modifications.

2.4.2.1 By using porous packings

Packed bed solar air heater absorbs solar radiation ‘in depth’ and has high ratio of heat transfer are to volume and high heat transfer capability, resulting in relatively low absorber temperature. This results in an increase in the efficiency of the solar collector. Enhancement of efficiency up to 60% at low flow rate (of the order of 0.018 kg/m^2-s) to about 45% at high flow rate (of the order of 0.04 kg/m^2-s) has been reported. Solar air heaters having a bed packed with slit and

expanded aluminum foil matrix, wire screen matrix, hollow spheres and crushed glass have been reported.

2.4.2.2 By increasing the area of heat transfer

Extended, corrugated and finned surfaces fall under this category. Bevil and Brandt (1968) described a solar air collector that consisted of 96 parallel and uniformly spaced aluminum fins placed below the glass cover plate. The results indicated that the efficiency of more than 80% could be obtained with the absorber having fins.

An experimental study conducted by Liu *et al.* (1984) to determine the temperature depression and increase in friction factor for an air heating flat plate solar collector by providing extended surface and concluded that the absorber plate temperature can be substantially lowered by using fins but accompanied by a significant increase in pressure drop.

Choudhury *et al.* (1993) carried out a detailed theoretical parametric analysis of a one pass, corrugated bare plate solar air heater. It was concluded that in order to obtain higher air temperature, lower air mass flow rate through the air heater and longer air channel is desirable.

2.4.2.3 By increasing convective heat transfer coefficient using fins and glass cover

Alta *et al* (2010) carried research on flat plate solar air heater using different designs such as with fins and without fins and with single glass cover and double glass cover they also made variation in mass flow rate and tilt angles. It was observed by this experiment that efficiency is more with fins than without fins; rise of temperature is more with lower air rate because of more time for heating, transparent cover decreases the convective heat losses. It was observed that energy efficiency increases with increase in mass flow rate while exergy efficiency decreases.

2.4.2.4 By increasing convective heat transfer coefficient using fins and multi pass

Naphon (2004) had numerically studied the performance and entropy generation of the double pass flat plate solar air heater with longitudinal fins. The effect of various parameters on heat transfer and entropy generation was investigated. In his model fins were attached upon absorber plate, by the investigation it was shown that with increasing number of fins, outlet air temperature and thermal efficiency both increases. With the increase in mass flow rate outlet air

temperature decreases, but thermal efficiency increases for corresponding number of fins. It is because heat transfer rate is directly proportional to mass flow rate. Thermal efficiency also increases with increasing fin height for same mass flow rate. Entropy generation rate is directly proportional to mass flow rate, but inversely proportional to height of fins as well as number of fins.

2.4.2.5 By increasing convective heat transfer coefficient using fins, multi pass and wire mesh

Omojaro and Aldabbagh (2010) observed experimentally thermal performance of a single and double pass solar air heater with fins and using a steel wire mesh as absorber plate. Porous media increases surface to volume ratio which results in improved thermal efficiency of solar air heater. With an increase in air mass flow rate efficiency increases and rise in temperature is low. It was clear from the experiment efficiency and temperature difference is more with double pass as compared with single pass. It was also observed that the efficiency also improves with lower height (between glass cover and upper channel).

2.4.2.6 By increasing convective heat transfer coefficient using artificial roughness

In order to attain higher convective heat transfer coefficient it is desirable that the flow at the heat transfer surface should be turbulent. However energy for creating turbulence has to come from the fan or blower and excessive turbulence means excessive power requirement. It is therefore, desirable that the turbulence must be created only very close to the surface, i.e., in laminar sub-layer only, where the heat exchange takes place and the core of the flow is not unduly disturbed to avoid excessive losses. Mittal (2007) carried out an experimental study on a flat plate air heater with absorber plate having thin wires used for creating artificial roughness. Experimental results showed that the rate of heat transfer in air heater with absorber plate having artificial roughness was considerably higher as compared to that in air an heaters with plane absorber.

Gupta and Kaushik (2009) had evaluated performance of solar air heater for various artificial roughness geometries. Artificial roughness breaks laminar sub layers disturbing the core to keep pressure drop within range. The effective efficiency suggest that roughness is required at high Reynolds number, but exergy based criterion suggest at very high Reynolds number exergy of

pump work required exceeds the exergy of heat energy collected by solar air heater. The investigation suggests that there was no roughened geometry which shows best exergy performance for whole range of Reynolds number. For smooth surface, circular ribs and V shaped ribs are suitable for smaller flow cross-section area of solar air heater duct and high Reynolds number.

2.4.2.7 By increasing convective heat transfer coefficient using obstacles

Cortes and Piacentini (2000) had developed a steady state mathematical model for a bare collector for heat transfer and friction in rectangular ducts with periodic disturbance and their effect on efficiency and pressure drop. In it a new term effective efficiency was used, which means extra heat obtained and additional amount of energy required moving air when obstacles were provided. Simulation was done for bare collector with or without perturbation. Both efficiency and effective efficiency depends on solar radiation intensity, collector dimensions, disturbance diameter and pitch. Efficiency was improved by increasing convective heat transfer coefficient for which we have to reduce duct equivalent diameter, increasing mass flow rate and increasing turbulence which result in increase of electric power supplied. While reducing the pitch there was increase in efficiency. Obstacles results in increase in the pumping power requirement for air. Perturbations increase effective efficiency of bare collector but it must be small, while pitch must increases with increases in mass flow rate.

2.5 Packed Beds

Packed beds are extensively used in chemical reactors, mass transfer system heat exchangers and heat storage equipment. Packing is of two types: regular or random. In the latter case, the bed has individual characteristics with respect to the surface area depending upon the method of packing. The fluid flow path in the case of packed beds is invariably tortuous. Hence, momentum and heat transfer equations applicable to fluid flowing in channels and ducts are not valid in case of packed bed ducts, much the same way as the criterion of laminar and turbulent flow of fluid in circular tubes and ducts is simply not applicable to packed beds. Packed beds offer the advantage of high heat transfer area to volume ratio, usually accompanied by high heat transfer coefficient.

High heat transfer rates due to larger area to volume ratio in packed bed solar collectors result in higher thermal efficiency.

2.6 Flow Regimes in Packed Beds

The bed porosity, P, is defined as the ratio of void volume to total bed volume. The mean interstitial mass velocity can then be expressed as the ratio of mass flow rate to porosity, G_o/P, and hence, the packed bed Reynolds number, Re_p by Kakac can be expressed as :

$$Re_p = 2 G_o D_e / 3(1-P)\mu \tag{2.18}$$

The characteristic length dimension, D_e, is taken as the diameter of the equivalent volume sphere. Mathematically, it is six times the packing volume (V_p) to packing surface area (A_p) ratio :

$$D_e = 6V_p / A_p \tag{2.19}$$

The hydraulic mean diameter of the flow passage can be expressed as:

$$D_h = 2D_e P/3(1-P) \tag{2.20}$$

Heggs has recommended the criteria for flow passages in packed bed as follows :

(a) For laminar flow regime

$$Re_p \leq 10 \tag{2.21}$$

(b) For transitional flow regime

$$10 \leq Re_p \leq 1000 \tag{2.22}$$

(c) For turbulent flow regime

$$Re_p \geq 1000 \tag{2.23}$$

2.7 Packed Bed Solar Air Heaters

Some of the important investigations on air heaters having packed bed are summarized below :

Sharma *et al.* (1991) has conducted experiments on collectors in which the space between the glass cover and bottom of the collector is filled with a number of slit and expended aluminum foils.

Three configurations were tested as follows:

(i) 17 layers of screens slightly compressed, filling up 25.4 mm space between glass cover and bottom.

(ii) 7 layers in the same space of 25.4 mm leaving a clearance 7.94 mm between glass cover and top of the foil stack.

(iii) The clearance between the glass cover and top of the foil decreased to 4.76 mm so that the 7 layers filled almost the total space.

The temperature rise in the three cases with the case where no foil is placed in the air flow passage is compared. It has been concluded that free air space between glasses and foil stack causes considerable portion of the air stream passing through this least resistance path. No significant change is observed in the temperature rise if the bed depth is reduced with completely filled up flow passage.

Chiou *et al.* (1977) have stated that a matrix type collector absorbs the solar radiation in depth and have high heat transfers area to volume ratio. Three possible flow namely unidirectional, cross flow and counter flow have been proposed. Unidirectional arrangement has been reported to have the important advantage of lower top losses resulting from a relatively cooler glass cover because it is in direct contact with the cool air. It result in higher thermal efficiency.

Experimental investigations of Sharma *et al.* (1991) on packed bed solar air heater having it's duct packed with blackened iron wire screen of different specifications as listed in Table 2.1 shows enhanced thermal performance. On the basis of experimental investigations it has been shown that the enhancement in thermal efficiency is a strong function of geometry of the wire mesh screen and operating parameters like insolation, inlet temperature and mass flow rate.

Table 2.1 specification of wire mesh screen matrices used Ahmad *et al*

(Bed depth = 25 mm)

Absorber	Mesh per cm	Wire diameter (mm)	No. of screens	Lateral pitch (mm)	Porosity
M1	2.16 × 2.16	0.528	12	4.618	0.953
M2	3.93 × 3.93	0.480	12	2.540	0.927
M3	4.53 × 4.53	0.528	12	2.208	0.898
M4	5.51 × 5.51	0.508	12	1.814	0.883
M5	3.15 × 3.15	0.712	12	3.175	0.873

Iron chips, aluminum chips and pebbles have been used as packing materials in solar air heaters by Mishra and Sharma (1981). Packed bed collector with iron chips has been found to be the most efficient due to higher $\sqrt{\alpha\kappa\rho C_p}$ (rate of flow of thermal energy into the surface of packing material). The high thermal diffusivity ($k/\rho C_p$) causes thermal energy to be absorbed rapidly, in comparison to non-metallic material (pebble).

Sharma *et al.* (1989) have studied the effect of porosity, thickness of bed and flow rate on the performance of packed bed air heater. The performance of packed bed air heater has been compared with those for smooth air heater.

Use of loosely packed iron turnings in the air heater in parallel flow arrangement has been investigated by Cheema and Mannan (1979). The effect of depth of absorber on performance has also been investigated.

Exact numerical solutions have been obtained for one dimensional steady state bed and fluid temperature distribution involving convective and radiative heat transfers by Beckman (1968). The following equations have been assumed to describe the temperature distribution of fluid and the porous bed in the absence of conduction.

Energy balance on fluid element:

$$C\frac{dT_f}{dx} - h_v(T_b - T_f) = 0 \qquad (2.24)$$

and energy balance on bed element yields :

$$S_o k e^{-kx/\mu_o} - \frac{dq_x}{dx} - h_v(T_b - T_f) = 0 \qquad (2.25)$$

Where C is fluid capacity rate

h_v is the volumetric heat transfer coefficient

S_o is the collimated flux making an angle with the x-axis which has cosine equal to μ_o.

k is the optical absorption coefficient

q_r is the net diffuse radiative flux parallel to the x-axis

These equations satisfy the boundary condition.

$$T_f(0) = T_i \qquad (2.26)$$

The governing equations are solved using following dimensionless parameters:

$$T_b^* = T_b / T_i \qquad (2.27)$$

$$T_f^* = T_f / T_i \tag{2.28}$$

$$\tau = k\,x \tag{2.29}$$

$$\Gamma = (C\,T_i)/(\sigma\,T_i^4) \tag{2.30}$$

$$\theta = (h_v T_i)/(k\sigma T_i^4) \tag{2.31}$$

$$\Psi = S_o/(\sigma T_i^4) \tag{2.32}$$

$$Q = q_r/(\sigma T_i^4) \tag{2.33}$$

Where, T_b^* and T_f^* represent dimensionless bed and fluid temperatures respectively.

τ is the optical depth

Γ is the dimensionless flow rate

θ is the dimensionless heat transfer coefficient

ψ is the dimensionless incident collimated heat flux at $\tau = 0$ and

Q is the dimensionless net diffuse radiative heat flux

The above equations are solved to give bed and fluid temperatures at specific locations. It has been reported that for optical depth of about 6, the bed and fluid temperatures are almost equal even for smallest value of dimensionless heat transfer coefficient.

Singh (1978) used iron shavings and wires as bed elements as well as absorbers for packed bed air heaters. Performance of these air heaters has been investigated experimentally with single glass cover, two glass covers having single pass and two pass flow arrangements. For single glass cover, air heater with iron shavings gives better performance than air heater with iron wires absorbers. This deviation of performance decreases at low temperatures of collection. Air heater with iron shavings absorber has a higher outlet temperature as compared to that with iron wire absorber, but in the evening after 3.00 p.m. precisely the reverse happens. This effect is

attributed to the fact that thermal capacity of iron wire absorber was more (18 kg iron wire) compared to iron shaving absorber (8 kg shavings) in the experiments conducted.

Choudhury and Garg (1993) have carried out theoretical analysis of solar air heating collectors of a conventional design having a glass cover along with absorber and back plate with air flow below the absorber plate and two different types of packed channel air heaters one like conventional type with packing in air flow passage between absorber and back plate and another consisting of two glass covers and back plate with blackened absorption packing between inner glass cover and back plate. The steady state energy balance equation for different components of the three types of air heaters are solved along with the boundary conditions to predict outlet temperature and efficiency based on outlet air temperature has been obtained.

Choudhury *et al.* (1988) have presented the results of studies similar to Choudhury and Garg (1993) on conventional bare plate collector without packing in the air duct (I type), packed bed collectors with non absorber packing beneath the absorber without cover (II type) and another packed bed collector with absorbing packing beneath a single cover (III type). Performance and pumping power of these collectors have been compared. Collector of type III has been found to be most efficient followed by type II. It has been reported that at 100 kg/hr m^2 of air flow rate, the optimized design corresponds to collector of 1-2 m length, duct depth of 10-15 cm and packing diameter of 3-5 cm.

Solar air heater packed with semi-transparent materials like glass beads or glass tubes have been investigated both experimentally and analytically by Hasatani *et al.* (1985). The experiments were conducted by modeling the radiative heat source for which eight infrared lamps (100 V – 125 W) were used. The lamps were arranged in two rows obtaining uniform flux above the glass cover. The collector used had the test section of size 1 m × 0.1 m × 0.3 m. The solution of energy balance equation developed for bed showed that the solar air heater with packed bed has higher efficiency of energy collection in comparison with that for a conventional flat plate collector.

Sodha *et al.* (1982) have analytically investigated the thermal performance of a matrix solar air heater. The heat balance equations on matrix element have been formulated and solved.

The following conclusions have been drawn from the work carried out:

1. The efficiency of system is a function of air mass flow rate and it increases with the increase of mass flow rate.
2. The matrix length to area ratio of the system is a sensitive parameter up to a critical value, beyond which the performance of the system does not change appreciably.
3. Increased absorption of insulation per unit length of the system decreases the efficiency.

Demirel and Kunc (1987) carried out experimental studies on a solar air heater with air flow channel underneath the absorber plate. The two cases were considered; one with empty flow channel and the other with channel packed with Rasching rings made of hard plastic. The instantaneous efficiency increases considerably when the packing of Rasching ring is used. Use of Rasching rings has been recommended because it does not cause excessive pressure drop in the system. Authors also analysed these collectors analytically. Based on this study it has been reported that the agreement between the measured and predicted performance is satisfactory for the first type, while it is relatively poor for the second type of collector.

Prasad and Saini (1993) carried out studies on air heaters packed with wire mesh screen matrix in unidirectional as well as cross flow arrangements. It has been reported that packed bed with unidirectional arrangement has higher efficiency as compared to that of the cross flow type. It has also been reported that thermal performance of packed bed collector is a strong function of porosity, extinction coefficient, heat transfer area density and the orientation of packing.
Experimental investigations have been made by Ahmad *et al.* (1996) on solar air heaters with iron screen matrix of different geometrical parameters as packing material in cross flow fashion. Specifications of matrices investigated are listed in Table 2.2. Thermohydraulic performance has been evaluated and compared with that of the smooth collector. It has been observed that thermohydraulic efficiency of packed bed air heater decreases with increase in the value of bed depth to element size ratio and porosity but it increases with increase in mass flow rate of air.

Table 2.2 Specifications of matrices used Ahmad et al

Absorber Type	**Mesh per cm**	**Wire dia. (mm)**	**Porosity**	**Bed depth/ element size**	**Packing surface area (m^2)**
M1	11.8 × 11.8	0.17	0.968	71.3	11.976
M2	7.8 × 7.8	0.27	0.946	53.3	13.500
M3	4.7 × 4.7	0.63	0.830	19.2	17.750

J.S.Saini (2004) conducted tests to cover wide range of influencing parameters such as geometrical and thermo physical characteristics of absorber matrix, mass flow rate and solar intensity and then results have been compared with those of flat plate collector. From these experiments copper woven screen was found to be best absorber matrix for packed bed solar air heater. Also the performance of collector improves appreciably as a result of packing its duct with blacked absorber matrix. For iron screen matrix the thermal efficiency is minimum and maximum with copper screen at lowest as well as highest mass flow rate.

Xu *et al* (2006) had developed method which studies the laminar flow and heat transfer at pore level. Using water as coolant, various configuration of wire screen mesh are investigated for their effect on heat transfer and pressure drop. In this investigation copper wire are used as packing material. The domain was first defined and then solved by Gambit and Fluent. During the study it was observed that, if Reynolds number is more than 2000 the pressure drop becomes more or less constant. The optimum value for porosity is 0.8. The decrease of the porosity is because of thickening of wire struts, which leads to greater flow acceleration due to the blockage by the

thickened struts. Then, this flow acceleration increases the heat transfer in both end wall and strut surfaces, but a further decrease of the porosity causes an increase of the thermally less-active dead flow region at the downstream side of the struts, leading to an overall reduction in the heat transfer. For particular porosity, heat dissipation rate increases as the surface area density increases. With the increase in porosity solid conduction increases and convection decreases.

2.8 Thermohydraulic Optimization of Solar Air Heater

As discussed earlier, the heat transfer coefficient of solar air heaters can be increased by providing artificial roughness on the rear side of the absorber plate or by packing the duct with matrices, leading to higher collector efficiency. Use of artificial roughness or porous material in the duct to enhance thermal performance of solar air heaters, however, results in higher friction factor and consequently a higher pumping power. It is, therefore necessary to optimize the system to maximize heat transfer while keeping frictional losses at the minimum possible level.

Cortes and Piacentini (2000) have suggested that performance of solar collector cannot be optimized by simply subtracting the electrical power from the thermal output of the collectors, because the former is produced mainly from thermoelectric sources and then transmitted, losing a considerable part of the energy in conversion and transmission. In order to evaluate the real economic performance of the collector, the effective efficiency is expressed by the following expression:

$$\eta_{eft} = \frac{q_u - \frac{P_m}{C}}{I A_c} \tag{2.34}$$

Here $C = \eta_f \eta_m \eta_{tr} \eta_{th}$ is the conversion factor accounting for net conversion efficiency from thermal energy of the resource to mechanical energy.

η_f is the efficiency of fan

η_m is the efficiency of electric motor used for driving fan

η_{tr} is the efficiency of electrical transmission from power plant

η_{th} is the thermal conversion efficiency of power plant

The value of C as suggested by Cortes and Piacentini (2000) is 0.18.

Paul and Saini (2004) tried to optimize packed bed collectors, one with wire mesh screen matrix bed and other with pebble bed on basis of minimum cost per unit energy delivered. There were two criteria's by which optimization can be achieved. These criteria's were maximum thermal efficiency or the minimum cost of unit energy delivered by the solar energy system, but the investigation was done with unit energy cost, because it considers pumping losses into account. The optimum design values at various solar intensities, porosity, pitch, diameter and number of layers for both wire mesh and pebble bed arrangements were obtained.

$$C_{sa} = (C_c A_c + C_e)I + P_a C_p + C_{mm} + C_{ml} \tag{2.35}$$

$$I(i, N) = \frac{i(1+N)^N}{(1+i)^N - 1} \tag{2.36}$$

Cost of solar energy system, Rs/year

Where I is the fraction of initial investment to be charged as investment and depreciation

N life span of the solar energy system, years

Chapter 3

Development of mathematical model

3.1 Introduction

Packed bed solar air heaters are known to perform efficiently in comparison to the conventional solar air heaters because they have high heat transfer area to volume ratio and tortuous air flow path for air to produce higher turbulence which provides rapid exchange of heat. In such air heaters the matrix absorbs the solar radiation in depth, which also results in high heat transfer capability and lower operating and matrix surface temperature. Thus, the thermal losses are substantially reduced resulting in improved thermal efficiency of packed bed air heater. An attempt to enhance heat transfer is always accompanied with increase in pressure drop and thus pumping power requirement is increased. It is therefore necessary to optimize the system to maximize heat transfer while keeping frictional losses at minimum possible level.

A methodology for optimization of packed bed solar air heater having their flow passage packed with wire screen matrices, has been presented in this chapter. For optimization the system, set of matrices are those used by Varshney and Saini (1998). The geometrical parameters of the matrix used are tabulated in Table 3.1. The Schematic diagram of the system used and the geometry of the wire screen used for making matrix inside the flow duct are shown in Figure. 3.1 and 3.2 respectively.

For the calculation of heat transfer and friction factor, the following correlations have been used as reported by Varshney and Saini (1998).

$$J_h = 0.647\left[\frac{1}{nP}\left(\frac{p_t}{d_w}\right)\right]^{2.104} Re_p^{-0.55} \tag{3.1}$$

$$f_p = 2.484\left[\frac{1}{nP}\left(\frac{p_t}{d_w}\right)\right]^{0.699} Re_p^{-0.44} \tag{3.2}$$

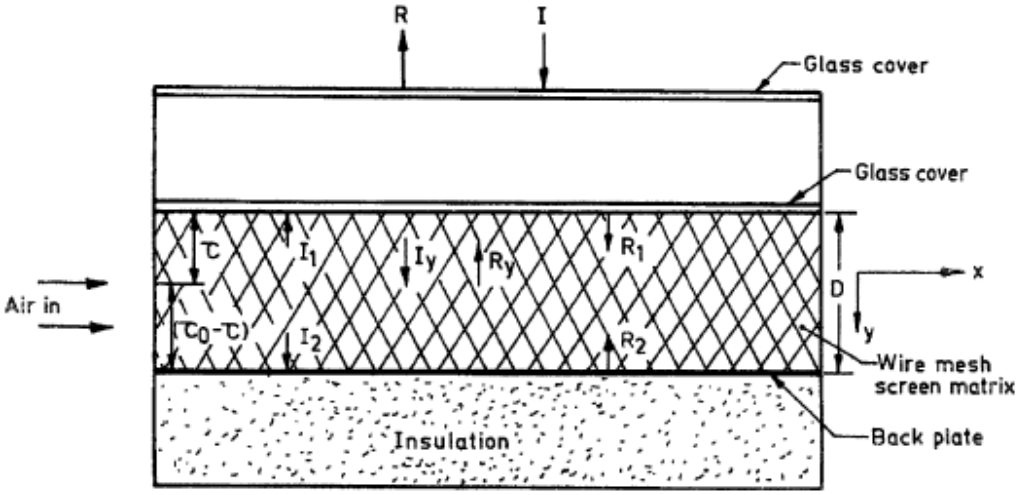

Fig 3.1 Schematic of packed bed solar air heater

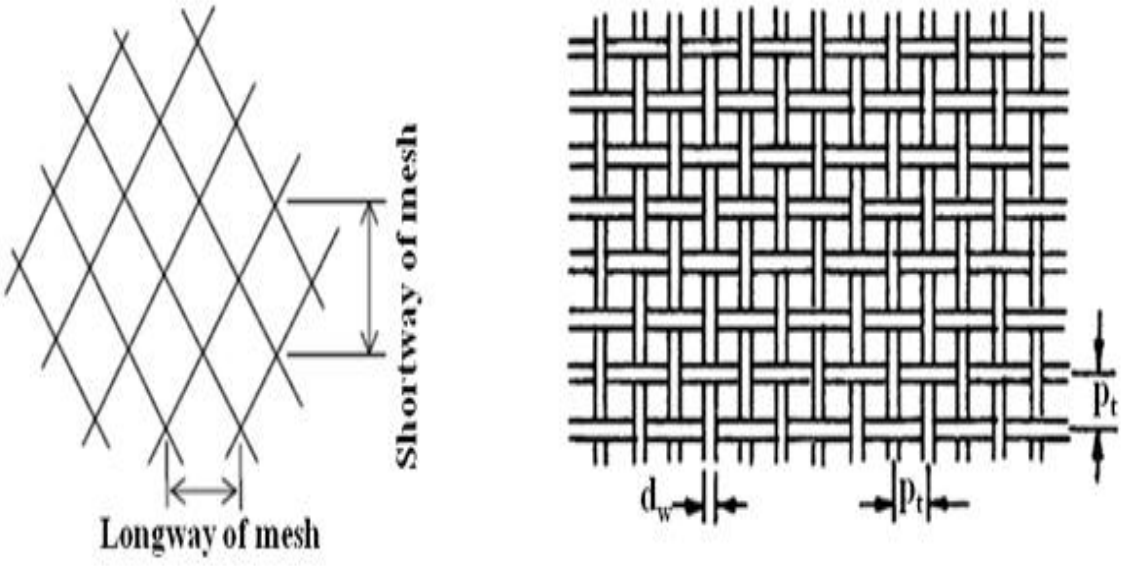

Fig 3.2 Wire screen geometry used as packing element

Table 3.1 Geometrical parameters of wire screen matrix Varshney and Saini

Matrix type	Wire dia. of matrix d_w (mm)	Pitch, p_t (mm)	No. of layers, n	Porosity P	Hydraulic radius, r_h	Extinction coefficient, β
M1	0.360	2.72	14	0.958	2.057	170.4
M2	0.450	2.08	10	0.939	1.725	210.8
M3	0.590	2.23	10	0.902	1.403	224.3
M4	0.795	3.19	9	0.887	1.575	181.2
M4(a)	0.795	3.19	7	0.905	2.023	142.6
M4(b)	0.795	3.19	5	0.937	2.994	102.4

3.2 Heat Transfer in the Bed

Heat transfer in the bed is assumed to take place by combination of conduction, convection and radiation. The details of each have been discussed below.

3.2.1 Heat Transfer by Conduction

Heat conduction in the direction of the air flow is assumed to be negligible. This has been reported by Chiou *et al.* (1965) and Hasatani *et al.* (1985). Conduction however takes place through contact surfaces of the matrix and lateral mixing of the fluid. Effective thermal conductivity has a complex relationship with the thermo-physical properties, type of matrix material, porosity and black paint used Chiou and Kunii. Effective thermal conductivity expression takes into account the effect of radiation heat exchange between the packing material and the surroundings.

Expression of effective thermal conductivity, k_e developed by Yagi and Kunii (1960) with flowing fluid has been used which is given below:

$$k_e = k_e^o + (k_e)_t \tag{3.3}$$

Here k_e^o represents the effective thermal conductivity of the packed bed with motionless fluid and $(k_e)_t$ is the thermal conductivity caused by lateral mixing of the fluid. $(k_e)_t$ is represented as :

$$(k_e)_t = (\alpha'\beta')D_e C_p G_o \tag{3.4}$$

$(\alpha'\beta')$ for steel wire mesh screens has been used as 0.12 which is the average of total range 0.1 to 0.14 in which the value lies for different packing reported by Yagi and Kunii.

D_e is equivalent diameter of the sphere which is expresses as :

$$D_e = 6/a_v \tag{3.5}$$

a_v being the heat transfer area per unit volume of the matrix.

k_e^o has been calculated using the following equations by Hasatani

$$k_e^o = \frac{1+P^{1.3}}{\dfrac{1}{k_p + h_{rv}D_e P^{1.3}/(1-P^{1.3})} + \dfrac{1}{(k_g/\phi)+h_{rs}D_e}} + \frac{16(n')^2\sigma T_b^3}{3\beta}$$

$$+ \frac{4h_{rv}P^{1.3}D_e k_p}{k_p + h_{rv}D_e P^{1.3}/(1-P^{1.3}) + (k_g/\phi) + h_{rs}D_e} \tag{3.6}$$

Here, k_p and k_g are the thermal conductivities of matrix material and air respectively.

ϕ is the ratio of effective thickness of fluid film adjacent to the contact surface of the two solid particles to mean diameter of solid. Numerical value of ϕ is taken as 0.12 Sharma (1990).

h_{rv} and h_{rs} are the heat transfer coefficients for thermal radiation from solid surface to solid and from void to void and can be expressed as Kunii:

$$h_{rs} = 0.1952 \left\{\varepsilon/(2-\varepsilon)\right\}\left\{T_b/100\right\}^3 \tag{3.7}$$

$$h_{rv} = \left[0.1952 \Big/ \left\{1 + \frac{P}{2(1-P)}\frac{1-\varepsilon}{\varepsilon}\right\}\right]\left(\frac{T_b}{100}\right)^3 \tag{3.8}$$

3.2.2 Heat Transfer by Convection

Convection mode contributes the maximum heat transfer in the matrix under low temperature operating conditions. Convective heat transfer is significant between the following:

i) Cover glass and the ambient air
ii) Cover glass and the air flowing in the duct
iii) Matrix and the air flowing inside the matrix, and
iv) Collector plate and air flowing above it

3.2.3 Heat Transfer by Radiation

A part of the solar radiation which falls on the absorbing matrix is absorbed by the matrix and the remaining is either reflected or scattered. Radiation heat exchange is known to occur between:

(i) Matrix and the cover glass
(ii) Between adjacent voids in the bed
(iii) Part of the matrix which are directly exposed to each other

In the analysis involving radiation heat transfer, the following assumptions have been made:

(i) The packed bed is isotropically homogenous, semi transparent layer for incident radiation.
(ii) The effect of scattering is negligible.
(iii) The boundary surface and the packed bed are gray material and the effect of optical properties is independent of the wave length.

(iv) Effective thermal conductivity expression takes into account the effect of emission in layer.

(v) Losses from bottom have been neglected.

Based on the above assumptions, the following relations for radiocity R, and irradiation I, as shown in Figure. 3.3 have been written for the collector having double glass cover, based on transmitted and reflected radiation.

$$R = r_c I + I_1(\tau)_{eff} \tag{3.9}$$

$$R_1 = I(\tau)_{eff} + r_c I_1 \tag{3.10}$$

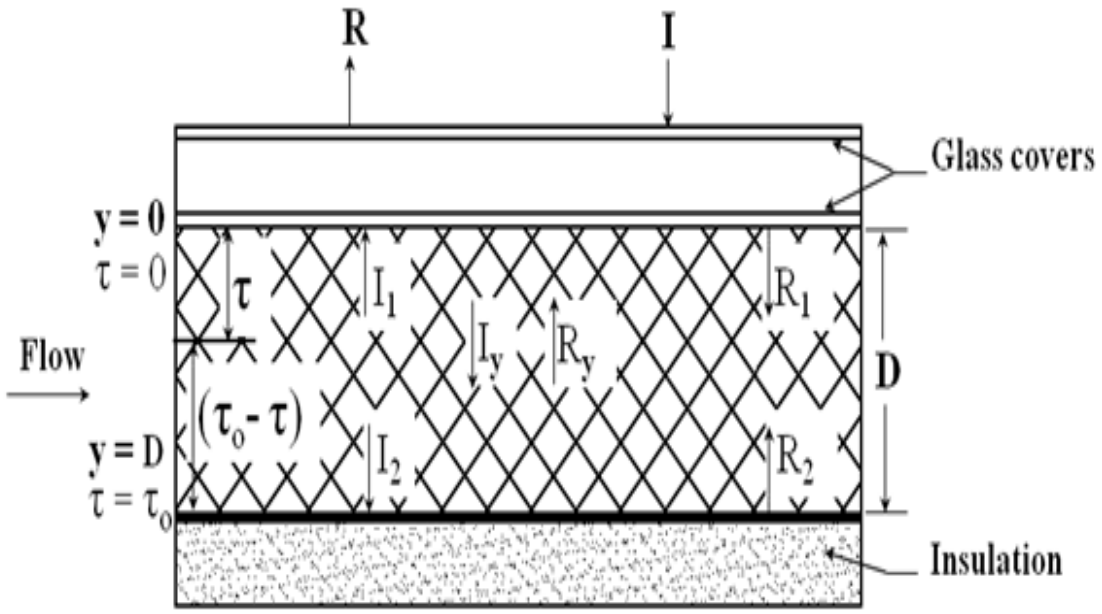

Fig 3.3 Radiative heat transfer in Bed

$$I_1 = R_2\, e^{-\tau_o} \tag{3.11}$$

$$I_2 = R_1\, e^{-\tau_o} \tag{3.12}$$

$$R_2 = (1-\varepsilon_p)\, I_2 \tag{3.13}$$

$$I_y = R_1\, e^{-\tau} \tag{3.14}$$

$$R_y = R_2\, e^{-(\tau_o - \tau)} \tag{3.15}$$

$$Q_r = I_y - R_y = R_1 e^{-\tau} - R_2 e^{-(\tau_o - \tau)} \tag{3.16}$$

Here, $(\tau)_{eff}$ is the effective transmittance for two cover glass system and τ is the optical depth of matrix.

Equation (3.10) can be rewritten substituting the values from Eqs. (3.11), (3.12) and (3.13).

$$R_1 = I(\tau)_{eff} \Big/ \left[1 - r_c(1-\varepsilon_p)e^{-2\tau_o}\right] \tag{3.17}$$

3.3 Governing Heat Balance Equations

Following the procedure of Hasatani *et al.* (1985) the heat balance equations for packed bed air heater have been written. The following assumptions have been made to simplify the analysis.

1. The temperature distribution within individual packing element and glass cover is uniform.
2. Conductive heat transfer in the flow direction is negligible.
3. Natural convection is not generated in the flow duct.
4. Physical properties of the packed bed material are independent of the temperature.
5. For the evaluation of the top losses, the value of top loss coefficient has been determined by Kleins equation (1975).

Heat balance equations have been modified for quasi steady state conditions in the analysis of the collector bed. While writing the heat balance equations, conduction losses through the side and back walls have been neglected. Further, the environmental temperature and wind velocity have been assumed uniform and constant.

The heat balance equations can be obtained as follows for the packed bed collector operating under actual outdoor conditions, as shown in Figure. 3.4(a) and Figure. 3.4(b).

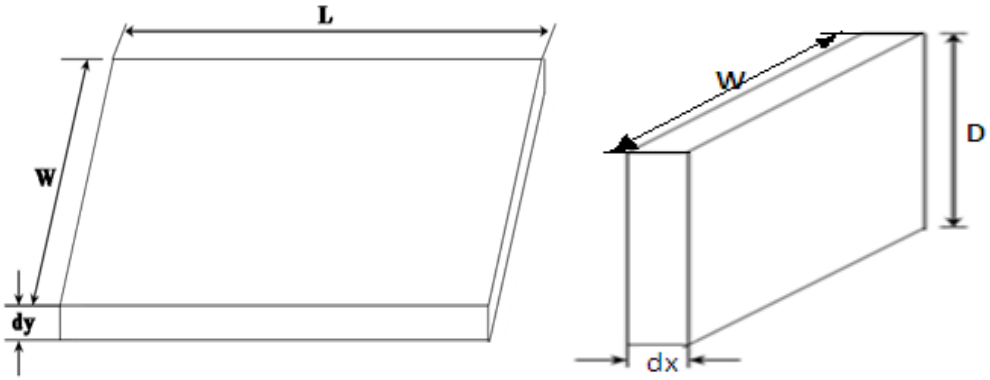

Fig 3.4(a) Energy Balance in matrix element along the (a) depth of bed and (b) along the length.

(Net heat flux entering the element due to conduction)

+ (Net heat flux due to radiation) = (Rate of heat gained by the air by means of convection from matrix to air) (3.18)

(Rate of rise in the sensible heat of air) = (Rate of energy carried away by the air) (3.19)

The mathematical expression of Eq. (3.18) using Fig. 3.4(a) can be written as:

$$\frac{\partial}{\partial y}\left[k_e \frac{\partial t_b}{\partial y} - Q_r\right] = h_c a_v \left(t_p - t_g\right) \tag{3.20}$$

The bed temperature t_b is assumed to be average of matrix temperature t_p and air temperature t_g. Therefore Eq. (3.20) can be rewritten as :

$$\frac{\partial}{\partial y}\left[k_e \frac{\partial t_b}{\partial y} - Q_r\right] = 2h_c a_v (t_b - t_g) \tag{3.21}$$

Similarly mathematical expression of Eq. (3.19) using Fig. 3.4(b) can be written as:

$$G_o C_p \frac{\partial t_g}{\partial x} = 2h_c a_v (t_b - t_g) \tag{3.22}$$

Applying boundary conditions for Eq. (3.21) the following additional equations are obtained:

at the top boundary i.e. at y = 0

$$k_e \frac{\partial t_b}{\partial y} - U_t(t_b - t_a) = 0 \tag{3.23}$$

at the bottom of bed i.e. at y = D

$$k_e \frac{\partial t_b}{\partial y} - Q_r = 0 \tag{3.24}$$

Boundary condition for Eq. (3.22) at the entry i.e. x = 0, can be written as:

$$t_g = t_i \tag{3.25}$$

3.3.1 **Non-Dimensionlisation of Differential Equations**

The following non-dimensional parameters are introduced in order to normalize the above equations:

$$\tau = \beta y \tag{3.26}$$

$$t_b^* = t_b / t_i \tag{3.27}$$

$$t_g^* = t_g / t_i \tag{3.28}$$

$$t_a^* = t_a / t_i \tag{3.29}$$

$$\bar{x} = x / L \tag{3.30}$$

$$h_v^* = 2h_v L / G_o C_p \tag{3.31}$$

$$h_v^{**} = 2h_v / k_e \beta^2 \tag{3.32}$$

$$Q_r^* = Q_r / k_e \beta t_i \tag{3.33}$$

$$U_t^* = U_t / k_e \beta \tag{3.34}$$

$$R_1^* = R_1 / k_e \beta t_i \tag{3.35}$$

$$R_2^* = R_2 / k_e \beta t_i \tag{3.36}$$

Using Equations (316), (3.35) and (3.36) following expression can be written:

$$Q_r^* = R_1^* e^{-\tau} - R_2^* e^{-(\tau_o - \tau)} \tag{3.37}$$

here, h_v is volumetric convective heat transfer coefficient which is calculated as :

$$h_v = h_c \, a_v \tag{3.38}$$

where h_c is convective heat transfer coefficient which is calculated from Eq. (3.1) and a_v is heat transfer area per unit volume of bed, which can be expressed as :

$$a_v = \frac{\text{Heat transfer area(A)}}{\text{Volume of bed}} = \frac{4A_f L(1-P)}{d_w (A_c D)} \tag{3.39}$$

Respective Eqs. (3.21) to (3.25) can be rewritten in the normalized form as under with the help of Eqs. (3.26) to (3.38). For convenience, we designate non-dimensional bed temperature t_b^* by u and non-dimensional air temperature t_g^* by v.

Hence, Eq. (3.21) can be written as:

$$\frac{\partial^2 u}{\partial \tau^2} - \frac{\partial Q_r^*}{\partial \tau} = h_v^{**}(u - v) \tag{3.40}$$

or

$$\frac{\partial^2 u}{\partial \tau^2} + R_1^* e^{-\tau} + R_2^* e^{-(\tau_o - \tau)} = h_v^{**}(u - v) \tag{3.41}$$

Boundary condition Eq. (3.23) is converted to:

$$\frac{\partial u}{\partial \tau} - U_t^*(u - t_a^*) = 0 \tag{3.42}$$

Other boundary condition Eq. (3.24) becomes:

$$\frac{\partial u}{\partial \tau} - Q_r^* = 0 \tag{3.43}$$

For air Eq. (3.22) can be written as:

$$\frac{\partial u}{\partial x} - h_v^*(u - v) \tag{3.44}$$

And it's boundary condition Eq. (3.25) will be:

$$v = 1 \tag{3.45}$$

Equations (3.41) to (3.45) are two dimensional non-linear partial differential equations which can be solved by finite difference method.

In order to cover a two dimensional region of the collector bed, a rectangular mesh is formed as shown in Figure. 3.5.

The height of the mesh is divided into (M-1) equal parts of length h and length into (N-1) equal parts of length k, therefore,

$$h = \tau_o/(M-1) \tag{3.46}$$

$$k = L/(N-1) \tag{3.47}$$

Using central difference in Eq. (3.41), forward difference in Eq. (3.42), backward difference in Eq. (3.43), backward difference in Eq. (3.44) and on rearranging, following equations are obtained.

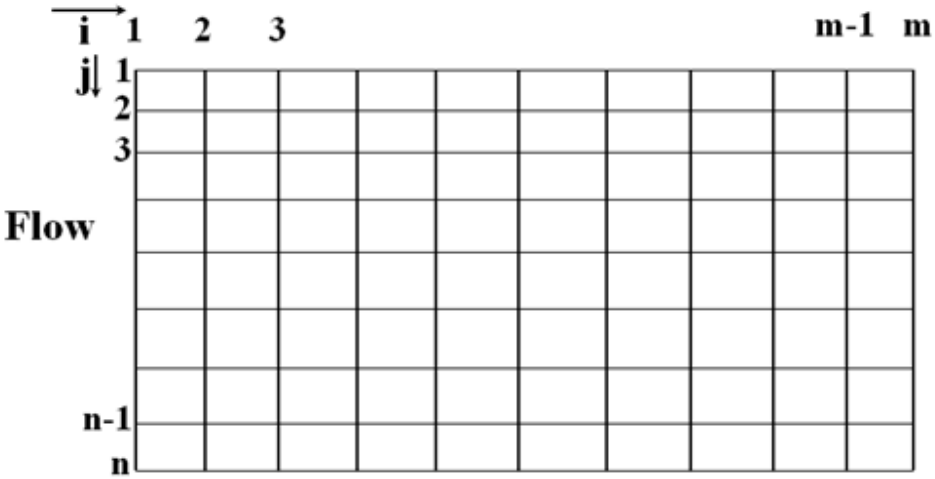

Fig 3.5 Grid layout of packed bed

$$u_{i,j} - \frac{1}{2 + h_v^{**}\, h^2}\, u_{i,j+1} - \frac{1}{2 + h_v^{**}\, h^2}\, u_{i,j-1} - \frac{h_v^{**}\, h^2}{2 + h_v^{**}\, h^2}\, v_{i,j} =$$

$$\frac{h^2}{2 + h_v^{**}\, h^2}\left[R_1^* e^{-(j-1)h} + R_2^* e^{-[\tau_o - (j-1)h]}\right] \qquad (3.48)$$

(valid for $1 \le i \le N$, $2 \le j \le M\text{-}1$)

$$u_{i,j} - \frac{1}{1 + hU_t^*}\, u_{i,j+1} = \frac{hU_t^* t_a^*}{1 + hU_t^*} \qquad (3.49)$$

(valid for $j = 1$, $1 \le i \le N$)

$$u_{i,j} - u_{i,j-1} = h\, Q_r^* \qquad (3.50)$$

(valid for $j = M$, $1 \le i \le N$)

$$v_{i,j} - \frac{1}{1 + k\, h_v^*}\, v_{i-1,j} - \frac{k\, h_v^*}{1 + k\, h_v^*}\, u_{i,j} = 0 \qquad (3.51)$$

(valid for $2 \le i \le N$, $j = M$)

$$v_{i,j} = 1 \tag{3.52}$$

(valid for $1 \le j \le M$, $i = 1$)

The constants in the above Eqs. (3.48) to (3.52) are substituted as given below:

$$C_1 = \frac{1}{1 + hU_t^*} \tag{3.53}$$

$$C_2 = hU_t^* t_a^* C_1 \tag{3.54}$$

$$C_3 = \frac{1}{2 + h_v^{**} h^2} \tag{3.55}$$

$$C_4 = h_v^{**} h^2 C_3 \tag{3.56}$$

$$C_5 = \frac{1}{1 + k h_v^*} \tag{3.57}$$

$$C_6 = k h_v^* C_5 \tag{3.58}$$

$$C_7 = h Q_r^* \tag{3.59}$$

$$H(j) = C_3 h^2 \left[R_1^* e^{-(j-1)h} + R_2^* e^{-[\tau_o - (j-1)h]} \right] \tag{3.60}$$

Substituting the constants, Eqs. (3.48) to (3.52) are written respectively as:

$$u_{i,j} - C_3 u_{i,j+1} - C_3 u_{i,j-1} - C_4 v_{i,j} = H(j) \tag{3.61}$$

(for $1 \le i \le N$, $2 \le j \le M\text{-}1$)

$$u_{i,j} - C_1 u_{i,j+1} = C_2 \tag{3.62}$$

(for $j = 1$, $1 \le i \le N$)

$$u_{i,j} - u_{i,j-1} = C_7 \tag{3.63}$$

(for $j = M$, $1 \le i \le N$)

$$v_{i,j} - C_5\, v_{i-1,j} - C_6\, u_{i,j} = 0 \tag{3.64}$$

(for $2 \le i \le N$, $1 \le j = M$)

$$v_{i,j} = 1 \tag{3.65}$$

(for $1 \le j \le M$, $i = 1$)

3.4 Solution of Equations

With the help of Eqs. (3.61) to (3.65), 2 (M × N) equations are written for the equal number of unknowns in the present analysis the values of M & N are taken as 10. These equations are solved to obtain non-dimensional bed and air temperatures. For solving the equations Gaurs Elimination method has been used.

3.5 Determination of Thermal Energy Gain (q_u)

The solution of Eqs. (3.61) to (3.65) gives non-dimensional bed and air temperatures which are converted to temperatures in degree Celsius. Average outlet temperature, t_o, is determined by averaging the air temperature at the nodal points corresponding to i = N.

Average outlet temperature is given by :

$$t_o = \frac{t_i \sum_{j=1}^{M} v_{i,j}}{M} \qquad \text{at } i = 1 \tag{3.66}$$

The rate of useful thermal energy gain of the collector can be expressed as follows :

$$q_u = \dot{m} C_p (t_o - t_i) \tag{3.67}$$

3.6 Determination of Pumping Power (P_m)

The mechanical power P_m, required to propel air through solar air duct is the product of volume flow rate Q and the pressure drop ΔP, across the duct expressed as:

$$P_m = Q\,\Delta P \tag{3.68}$$

The pressure drop across the duct of length, L can be written as:

$$\Delta P = \frac{f_p L \rho v^2}{2 r_h} \tag{3.69}$$

Where,

f_p is friction factor for packed bed, which is evaluated from Eq. (3.2)

ρ is density of air

v is velocity of air in duct which can be calculated as follows :

$$v = \frac{\dot{m}}{\rho A_f P} \tag{3.70}$$

Volume flow rate is given by :

$$Q = \frac{\dot{m}}{\rho} \tag{3.71}$$

3.7 Determination of Effective Efficiency

It is necessary to take into account the electrical energy required for pumping, while calculating the actual performance of solar air heater. Since the electrical power to drive the pump is usually produced from some thermal energy source, transmitted and then converted to mechanical energy, loosing always considerable part of the energy in conversion and transmission. Therefore, the pumping power required is converted to equivalent thermal energy to obtain net thermal output of the collector. Based on this criterion, Cortes and Piacentini (1990) evaluated

the actual performance of the solar collector in terms of the effective efficiency which can be expressed as :

$$\eta_{eft} = \frac{q_u - P_m / C}{I A_c} \tag{3.72}$$

Where C is the conversion factor accounting for net conversion efficiency from thermal energy of the resource to mechanical energy.

3.8 Computer Program

A computer program has been developed in C^{++} (given in Appendix) to compute the results. This program evaluates the coefficient of all the equations and then these coefficients are placed in the form of matrix. The solution of the matrix generates the non-dimensional bed and air temperatures. These non-dimensional temperatures are then converted to temperatures in degree Celsius. Average outlet air temperature is determined by averaging the air temperature at the nodal points corresponding to i = N. The average outlet temperature along with the mass flow rate is used to evaluate the thermal energy gain of the collector. Pumping power required to force air through the duct is determined by the friction factor correlation as given by Eq. (3.68). Equivalent thermal energy corresponding to required pumping power is subtracted from thermal energy gain of the collection to determine net thermal energy gain. The net thermal energy gain along with the insolation are used to determine the effective efficiency.

To illustrate the process a small size mesh (2 × 3) has been considered as shown in Fig. 3.7. A 2 × 3 sized mesh will have 2 × 3 = 6 nodal points and a total 2 (2 × 3) = 12 equations will be generated using Eqs. (3.61) to (3.65) for 12 unknowns (6 bed temperatures and 6 air temperatures at total 6 locations).

For i = 1, j = 1 [using Eqs. (3.62) and (3.65)]

$$u_{1,1} - C_1 u_{1,2} = C_2 \tag{3.73}$$

$$v_{1,1} = 1 \tag{3.74}$$

For i = 1, j = 2 [using Eqs. (3.61) and (3.65)]

$$u_{1,2} - C_3 u_{1,3} - C_3 u_{1,1} - C_4 v_{1,2} = H(j) \tag{3.75}$$

$$v_{1,2} = 1 \tag{3.76}$$

For i = 1, j = 3 [using Eqs. (3.63) and (3.65)]

$$u_{1,3} - u_{1,2} = C_7 \tag{3.77}$$

$$v_{1,3} = 1 \tag{3.78}$$

For i = 2, j = 1 [using Eqs. (3.62) and (3.64)]

$$u_{2,1} - C_1 u_{2,2} = C_2 \tag{3.79}$$

$$v_{2,1} - C_5 v_{1,1} - C_6 u_{2,1} = 0 \tag{3.80}$$

For i = 2, j = 2 [using Eqs. (3.61) and (3.64)]

$$u_{2,2} - C_3 u_{2,3} - C_3 u_{2,1} - C_4 v_{2,2} = H(j) \tag{3.81}$$

$$v_{2,2} - C_5 v_{1,2} - C_6 u_{2,2} = 0 \tag{3.82}$$

For i = 2, j = 3 [using Eqs. (3.63) and (3.64)]

$$u_{2,3} - u_{2,2} = C_7 \tag{3.83}$$

$$v_{2,3} - C_5 v_{1,3} - C_6 u_{2,3} = 0 \tag{3.84}$$

These 12 Eqs. (3.73) to (3.84) are solved in order to determine all the 12 unknowns i.e. bed and air temperatures at 6 locations. Coefficients of the equations are placed in matrix form as shown below:

$$\begin{bmatrix} 1 & 0 & -C_1 & 0 & 0 & 0 & 0 & 0 & 0 & 0 & 0 & 0 \\ 0 & 1 & 0 & 0 & 0 & 0 & 0 & 0 & 0 & 0 & 0 & 0 \\ -C_3 & 0 & 1 & -C_4 & -C_3 & 0 & 0 & 0 & 0 & 0 & 0 & 0 \\ 0 & 0 & 0 & 1 & 0 & 0 & 0 & 0 & 0 & 0 & 0 & 0 \\ 0 & 0 & -1 & 0 & 1 & 0 & 0 & 0 & 0 & 0 & 0 & 0 \\ 0 & 0 & 0 & 0 & 0 & 1 & 0 & 0 & 0 & 0 & 0 & 0 \\ 0 & 0 & 0 & 0 & 0 & 0 & 1 & 0 & -C_1 & 0 & 0 & 0 \\ 0 & -C_5 & 0 & 0 & 0 & 0 & -C_6 & 1 & 0 & 0 & 0 & 0 \\ 0 & 0 & 0 & 0 & 0 & 0 & -C_3 & 0 & 1 & -C_4 & -C_3 & 0 \\ 0 & 0 & 0 & -C_5 & 0 & 0 & 0 & 0 & -C_6 & 1 & 0 & 0 \\ 0 & 0 & 0 & 0 & 0 & 0 & 0 & 0 & -1 & 0 & 1 & 0 \\ 0 & 0 & 0 & 0 & 0 & -C_5 & 0 & 0 & 0 & 0 & -C_6 & 1 \end{bmatrix} \begin{bmatrix} u_{11} \\ v_{11} \\ u_{12} \\ v_{12} \\ u_{13} \\ v_{13} \\ u_{21} \\ v_{21} \\ u_{22} \\ v_{22} \\ u_{23} \\ v_{23} \end{bmatrix} = \begin{bmatrix} C_2 \\ 1 \\ H(J) \\ 1 \\ C_7 \\ 1 \\ C_2 \\ 0 \\ H(J) \\ 0 \\ C_7 \\ 0 \end{bmatrix}$$

The above matrix is solved by Gauss elimination method which gives the values of non-dimensional bed and air temperatures. The non-dimensional temperatures are converted to dimensional form using Eqs. (3.50) and (3.51).

Values of system and operating parameters used for evaluation of effective efficiency are given in Table 3.2.

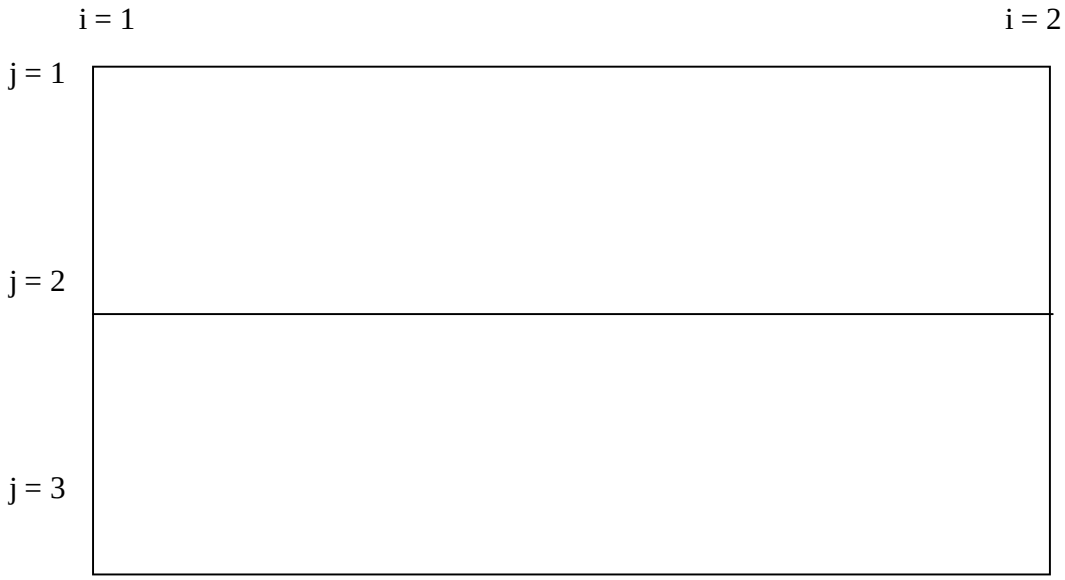

Fig. 3.6 Grid layout with M = 3, N = 2

Table 3.2. Numerical values of system and operating parameters used in analytical calculation

S.No.	***Input data***	**Numerical value**
1.	Length of collector, L	2.39 m
2.	Width of collector duct, W	0.41 m
3.	Depth of collector, D	0.025 m
4.	Mass flow rate of air, G	0.005 to 0.05 kg/s
5.	Insolation, I	700 W/m^2
6.	Inlet air temperature, t_i	35°C

7.	Ambient temperature, t_a	35°C
8.	Absorptivity of cover glass, α_c	0.13
9.	Reflectivity of cover glass, r_c	0.0434
10.	Emissivity of wire mesh screen, ε	0.8
11.	Emissivity of bottom plate, ε_p	0.8
12.	Thermal conductivity of matrix, k_s	62.764 W/m°C
13.	Thermal conductivity of air, k_a	0.0267 W/m°C
14.	Density of air, ρ	1.2 kg/m^3
15.	Refractive index of mesh material, n′	1.0
16.	Viscosity of air, μ	0.00001865 kg/m^3
17.	Wind heat transfer coefficient, h_w	10.0 W/m^2K
18.	Eff. Transmissivity of covers, $(\tau)_{eff}$	0.72

Chapter 4

Results & Discussion

Effective efficiency of different matrices has been obtained using the approach described in mathematical modeling for smooth as well as packed bed collectors. The analysis is done at constant value of solar isolation as 700W/m^2 and ambient air temperature as 35^0C by varying mass flow rate in range of 0.005 Kg/s to 0.05Kg/s. The result obtained by the mathematical modeling is discussed below.

4.1 Effect of Reynolds Number On Thermal Energy Gain And Pumping Power:

When Reynolds number is higher the gain in useful energy becomes constant, but the pumping power increases with the Reynolds number, it is clearly shown in Figure 4.1 which shows the effect of Reynolds number on thermal energy gain for matrix M2. From figure it is clear that at lower Reynolds number pumping power required to pump the air through the duct is low which increases with increase in Reynolds number. On the other hand useful energy gain increases with increase in Reynolds number but then it becomes constant at higher value. Figure depicts there is value of Reynolds number at which useful energy gain (Thermal energy gain minus pumping power) is maximum. Beyond or below this optimum value of Reynolds number net energy gain is less then compared to optimum value of Reynolds number.

4.2 Effect of Reynolds Number on Effective Efficiency:

Effective efficiency increases up to certain value with increase in Reynolds number and then it starts diminishing with further increase in Reynolds number as shown in Figure 4.2. With the increase in fluid flow rate maximum value of effective efficiency is achieved, there only one, optimum effective efficiency at particular Reynolds number for a particular matrices. From this it is evident that Reynolds number is crucial parameter that determine thermal energy gain, pumping power and effective efficiency.

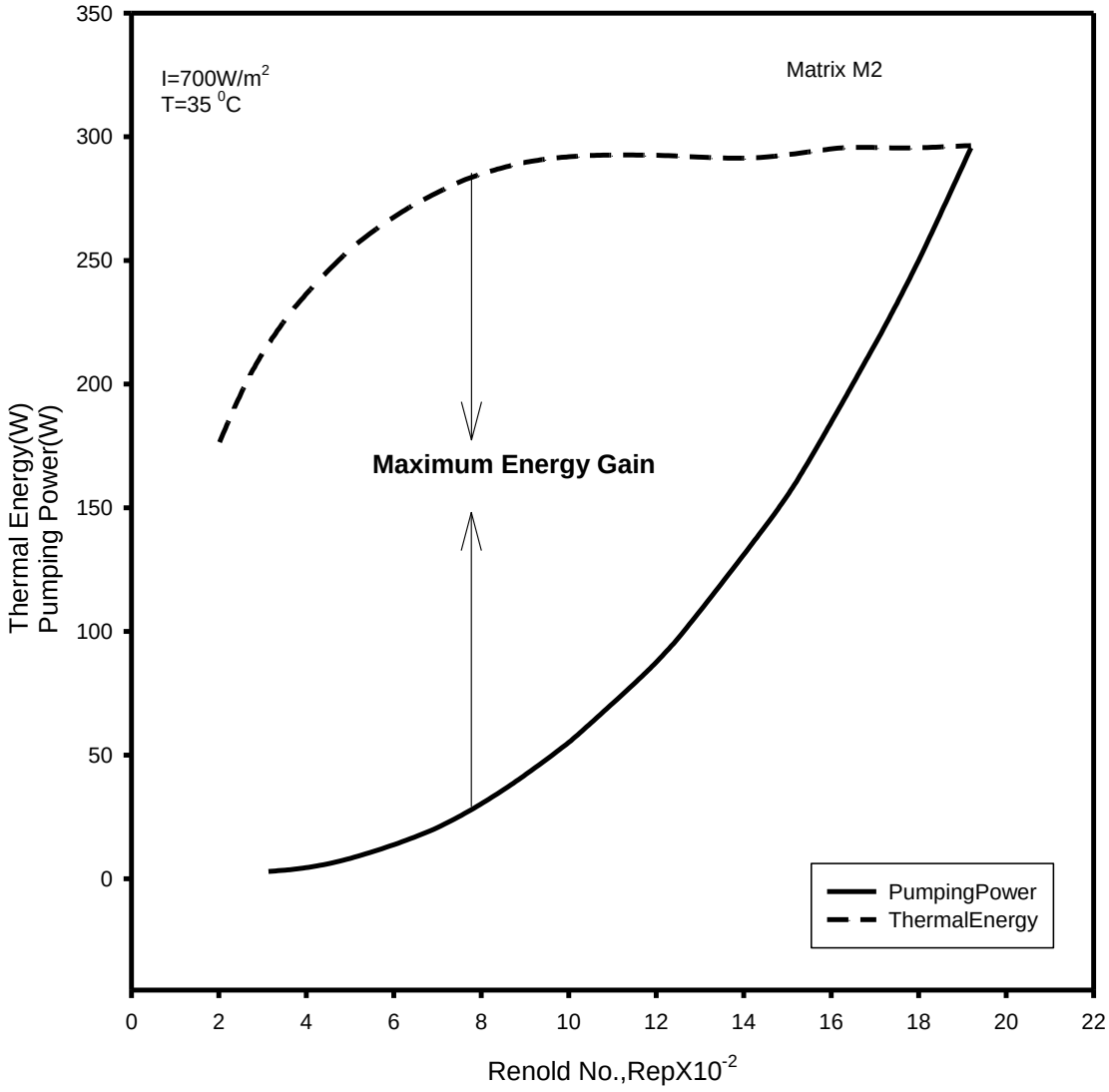

Fig. 4.1 Effect of Reynolds number on thermal energy and pumping power

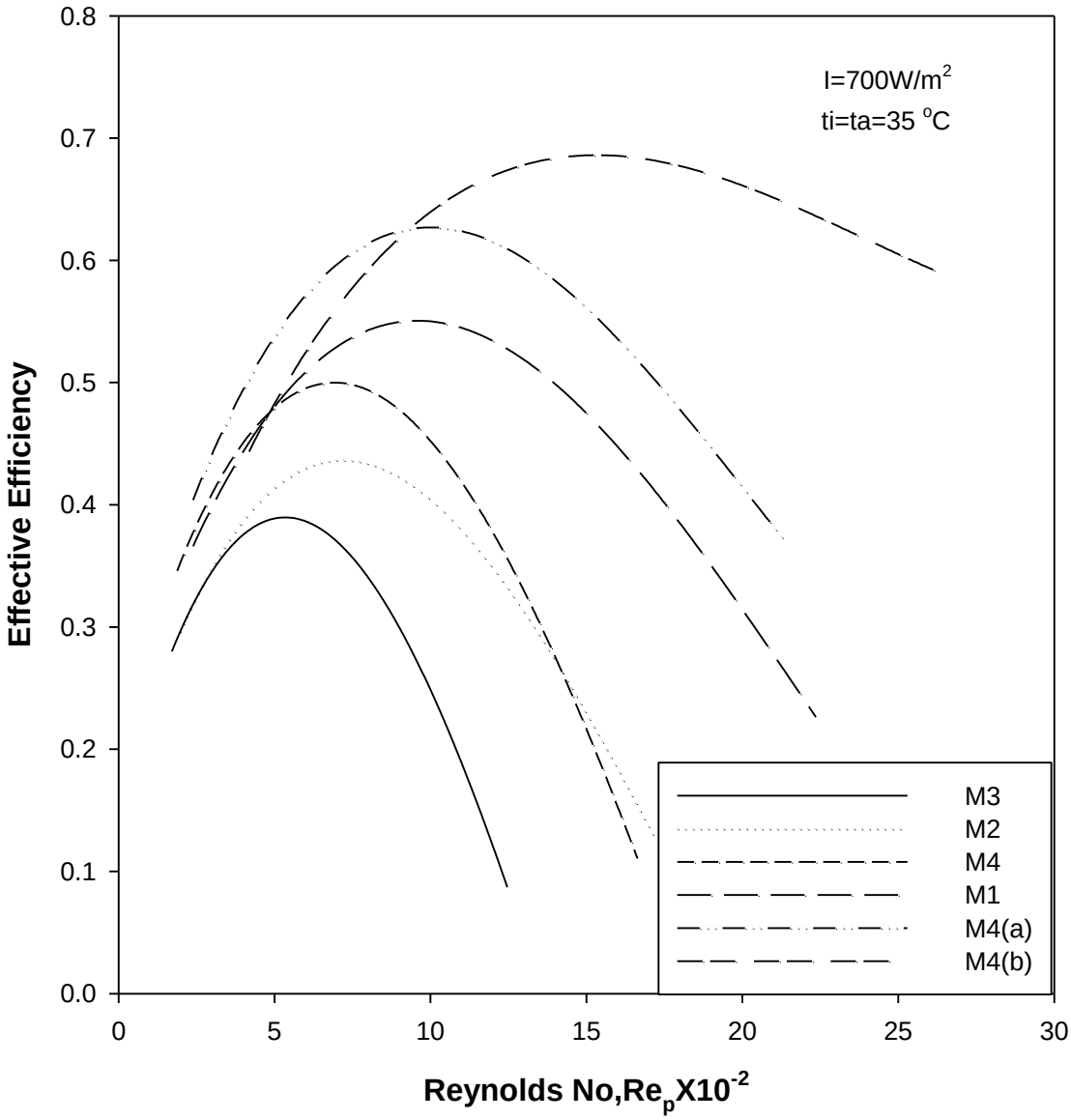

Fig 4.2 Reynolds number verses Effective Efficiency

4.3 Effect of Mass Flow Rate on Effective Efficiency:

Figure 4.3 depicts the comparison of effective efficiency of smooth solar air heater with packed bed solar air heater. There is difference in defining Reynolds number for packed bed solar air collector and smooth solar air collector, because of this reason the comparison is done on mass flow rate bases rather than on the basis of Reynolds number. Figure shows that above certain mass flow rate, basis the smooth solar air collector becomes more efficient than packed bed solar air collector, but on the other hand thermal efficiency of packed bed solar air collector is higher than smooth solar air collector. With in all these effective efficiency is higher while using M4(b) matrix as a packing material and lowest with M3 matrix. The variation of effective efficiency with respect to the mass flow rate is same as with respect to the Reynolds number.

4.4 Efficiency Verses Reynolds Number for different number of screens in fixed bed depth:

Mesh M3 and M4 (a) having same pitch but different geometry are plotted for effective efficiency verses Reynolds number in figure 4.4. It is observed that effective efficiency is highest for M4 (a) than M3 in whole range of Reynolds number in which they are tested. From this it is evident that geometry of matrix strongly affects the effective efficiency of solar air heater, but porosity alone does not have any effect on the performance of solar air heater.

4.5 Effective Efficiency Verses Reynolds Number on the basis of different number of meshes in fixed bed Depth:

In Figure 4.5 effective efficiency is drawn with respect to Reynolds number for meshes of same geometry but with different number of layers. It shows that with increase in number of layers of same geometry effective efficiency decreases. It is due to increase of friction losses with increase in layers consequently pumping power will also increases M4 with nine meshes has the least efficiency, while M4(b) with five mashes has the maximum efficiency and also on the widest range. Other reason for decrease in effective efficiency is with more number of screens they will be tightly pressed against each other effective heat transfer area will reduces.

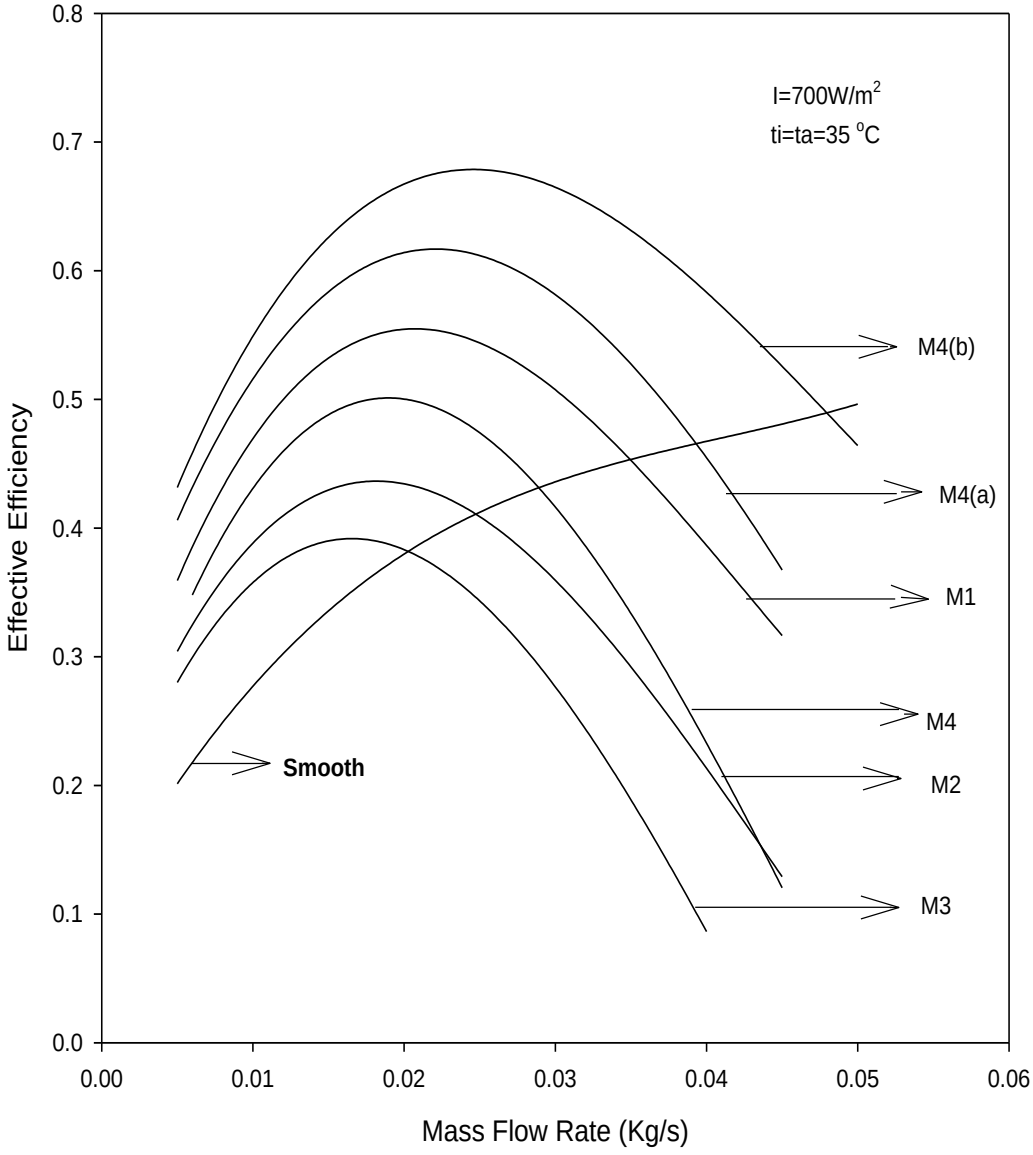

Fig 4.3 Reynolds number verses Effective Efficiency

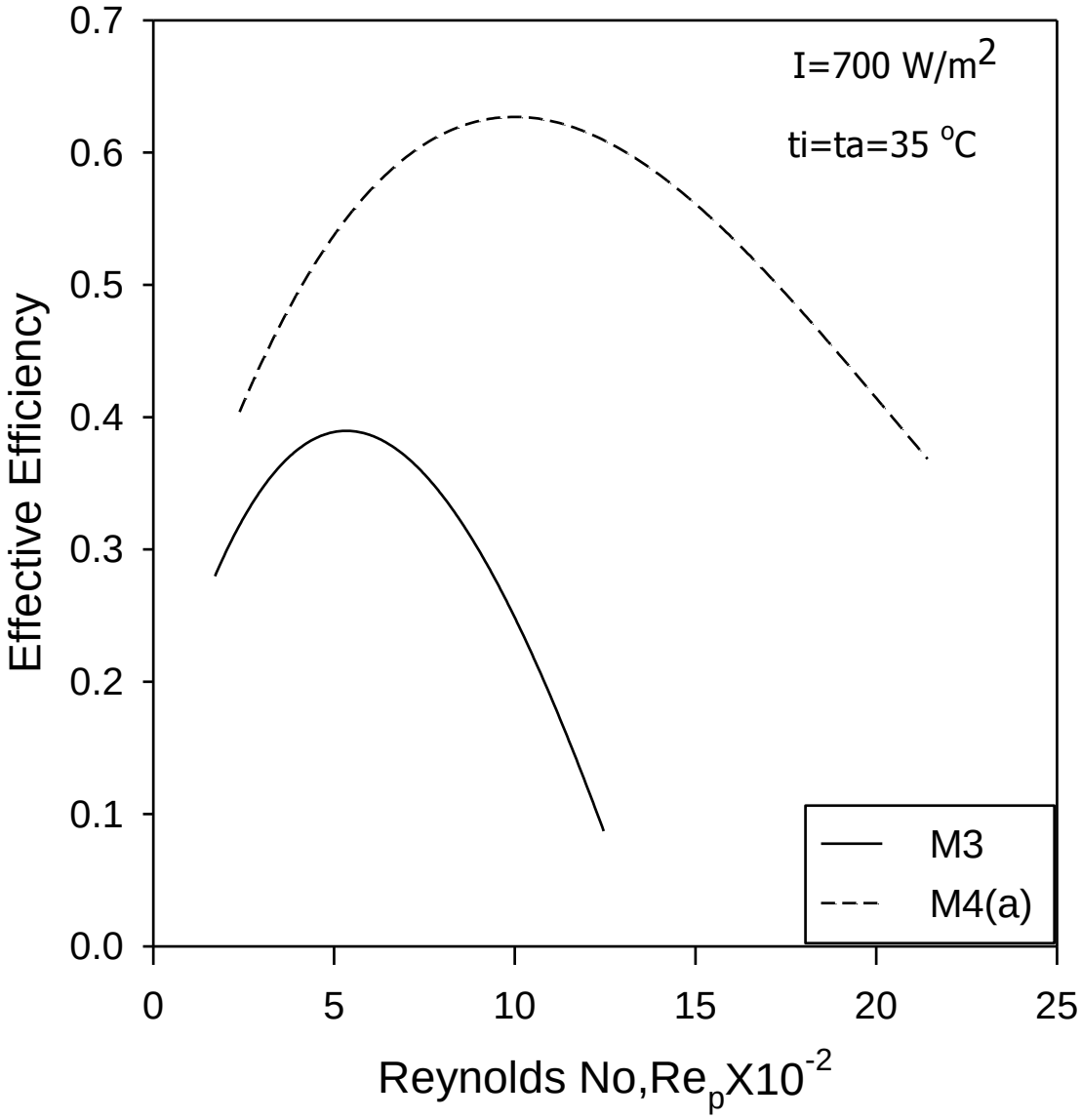

Fig 4.4 Reynolds number verses Effective Efficiency

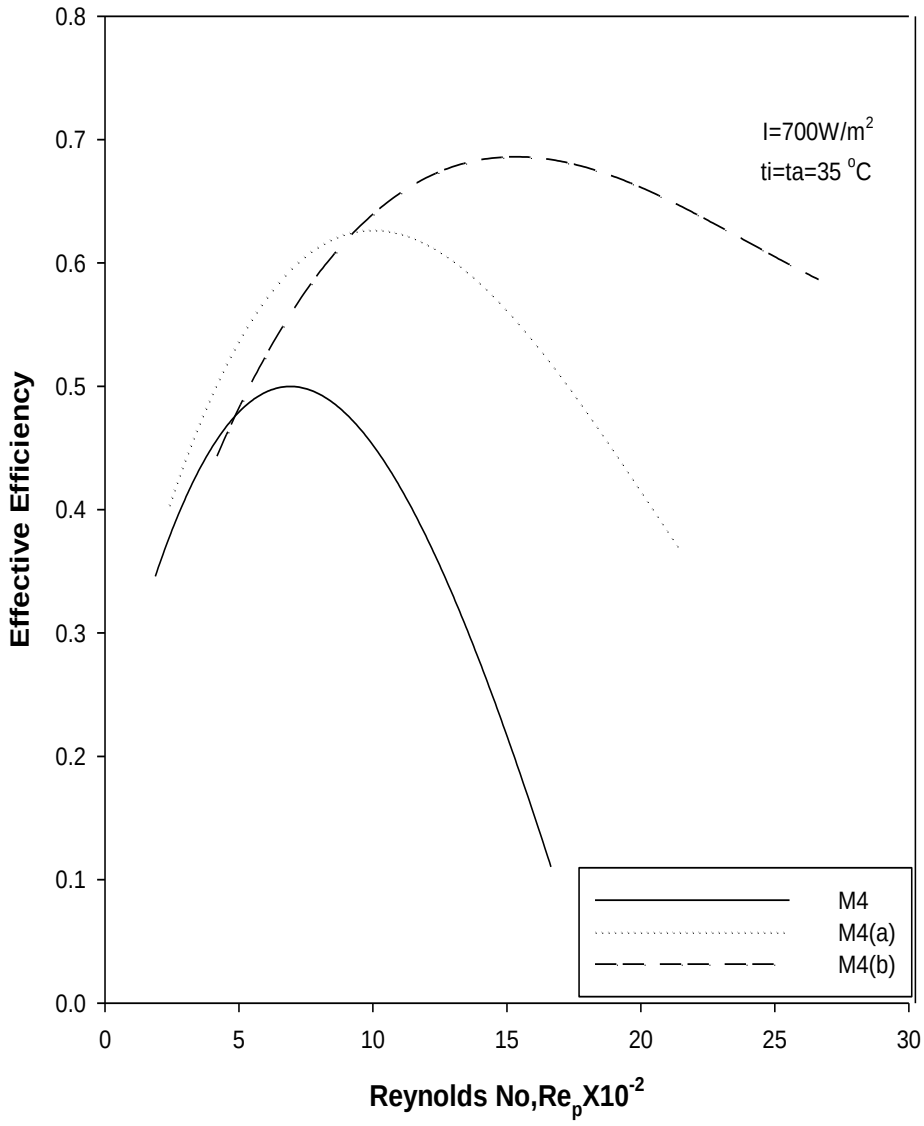

Fig 4.5 Effective Efficiency verses Reynolds number having different number of Mesh screen in fixed bed depth.

4.6 Effective Efficiency Verses Temperature Rise Parameter :

The plot between effective efficiency and temperature rise parameter for different types of matrices is drawn in figure 4.6. When mass flow rate increases then temperature rise parameter decreases because of temperature rise is inversely proportional to mass flow rate. As the temperature rise parameter decreases, first effective efficiency increases and then starts diminishing. In case of low temperature rise parameter smooth solar air collector is more efficient than any packed bed collector. It also shows that effective efficiency increases moderately with decreases in temperature rise parameter in higher ranges, where as in lower value of temperature rise parameter the effective efficiency decreases sharply. The reason for this trend is based on the fact that for lower flow rate rise in temperature shall be higher while the fractional losses would be lower, resulting in higher effective efficiency, when the temperature rise is low then the mass flow rate is higher, then frictional losses would increases due to this more pumping power is required, this would ultimately reduces effective efficiency at larger flow rates.

4.7 Thermal Efficiency Verses Temperature Rise Parameter :

Figure 4.7 which have been drawn between thermal efficiency and temperature rise parameter for various matrices and smooth flow solar air heater. From this figure it was observed that smooth solar air heaters are never thermally more efficient than packed bed solar air heater. It was observed that with rise in temperature rise parameter thermal efficiency starts diminishing. When temperature rise parameter is low thermal efficiency of any kind of solar heater is higher than other ranges.

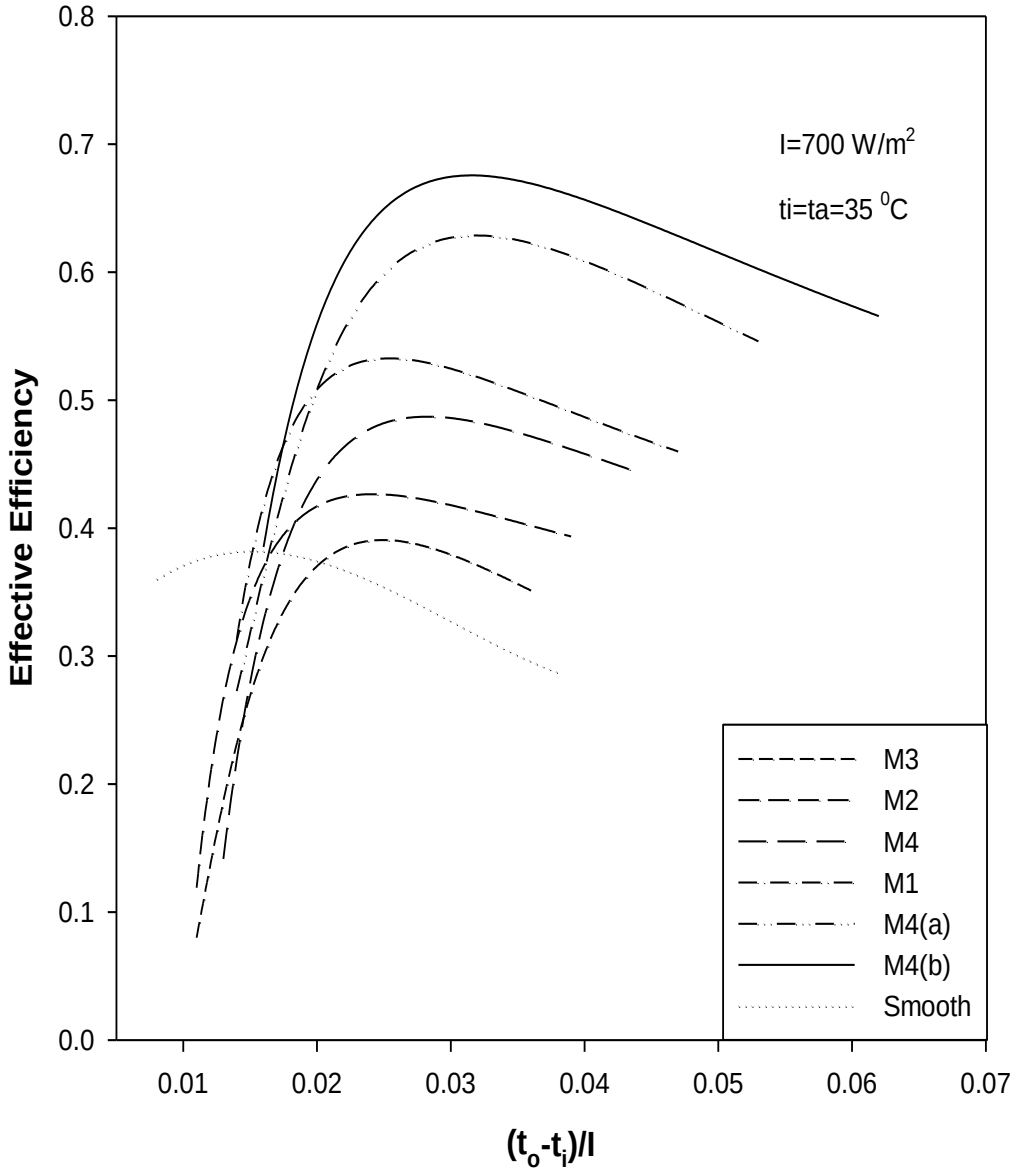

Fig. 4.6 Effective Efficiency verses Temperature rise parameter

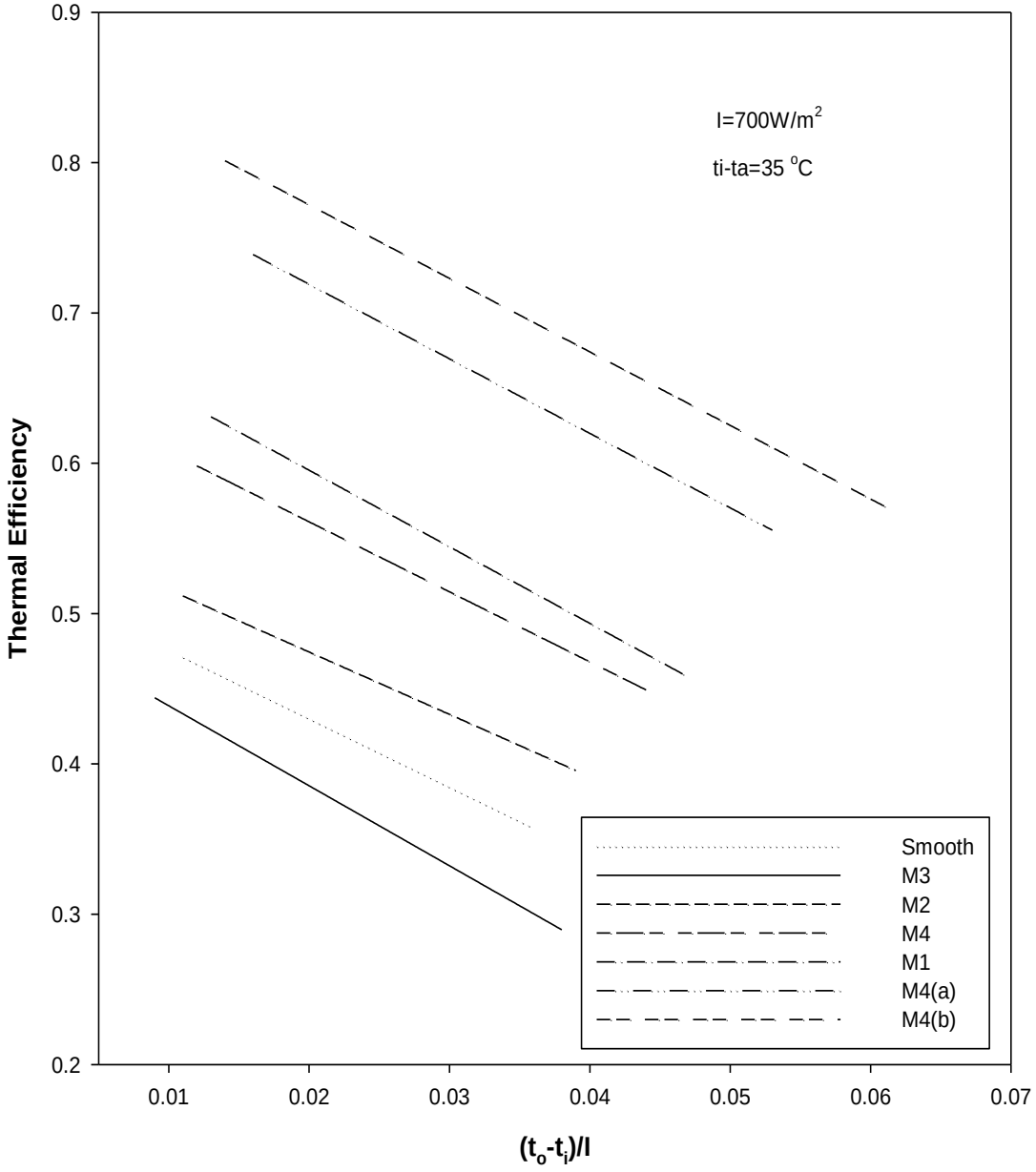

Fig 4.7 Temperature Rise Parameter verses Thermal Efficiency

4.8 Design Criterion

It has been shown that thermal efficiency as well as effective efficiency is a function of geometrical parameters of the matrix in packed bed air heater. Therefore it is desirable to select the best geometry of matrix which results in best performance of the collector under given set of performance and given set of conditions. From figures 4.6 and 4.7 it is clear that for higher value of temperature rise parameter the effective efficiency and thermal efficiency trends are similar and for designing a matrix packed solar air heater design parameter can obtain on the basis of thermal performance. In most of practical applications, solar air heater is operated in this temperature rise parameter range. However, for any specific application of the air flow rates are desired, then the designed parameters are to be based on effective efficiency. However, low range of temperature rise parameter is not recommended since the frictional losses predominate in this range.

A method for determining the design parameter for a solar air heater of known dimensions and characteristics, operating under different operating conditions, is based on the recommendation of Reddy and Gupta. In this method, a graph for thermal efficiency is plotted against temperature rise parameter. With the help of this plot, mass flow rate can be determined for a desired temperature rise and efficiency needed for a particular application at a specific location where the intensity of solar radiation is known.

Chapter 5

Conclusions

1. The thermohydraulic investigation of packed bed solar air heater packed with wire screen matrix shows that thermal gain of such collector is relatively higher as compared to smooth collector, but at the same time, the pressure drop across the duct also increases significantly.
2. The Reynolds number has been found to be a strong parameter affecting the effective efficiency. It has been found there exists an optimum vale of effective efficiency for a given matrix.
3. Beyond a certain value of mass flow rate, the smooth collector is found to be more thermohydraulically efficient as compared to packed bed collector. Solar air heater with matrix M4(b) is found to yield best thermohydraulic efficiency in operating range of mass flow rate 0.005 Kg/s to 0.035 Kg/s.
4. It is found that for higher value of temperature rise parameter, the effective efficiency values closely follow the thermal efficiency values, where there is appreciable difference in the lower range of temperature rise parameter values.
5. It has been observed that effective efficiency of a packed bed air heater strongly depends on the parameters of matrix. Merely porosity of bed does not govern the performance.

References

1. Agarwal, V.K. and Larson, D.C.,(1981). Calculation of top loss coefficient of a flat plate collector, *Solar Energy*, **27**, 69-71.
2. Ahmad, A., Saini, J.S. and Varma, H.K.,(1996). Thermo-hydraulic performance of packed-bed solar air heater, *Energy Convers, Mgmt.* **37** (2), 205-214.
3. Ahmad, A., (1995). Studies on the performance of packed bed solar air heaters, Ph.D. Thesis, Department of Mechanical and Industrial Engineering, University of Roorkee, Roorkee.
4. Akhtar, N. and Mullick, S.C., (1998). Prediction of Glass cover temperature of solar collector with single glazing, *SESI Journal*, **8** (1), 11-25.
5. Akpinar, Ebru Kavak., Kocyigit, Fatih., (2010). Energy and exergy analysis of a new flat-plate solar air heater having different obstacles on absorber plates, Applied energy,3438-3450.
6. Akpinar, Ebru Kavak., Kocyigit, Fatih.,(Dec 2010). Experimental investigation of thermal performance of solar air heater having different obstacles on absorber plates, Heat and Mass Transfer,416-421.
7. Alta, Deniz., Bilgili, Emin., Ertekin, C., Yaldiz, Osman., (2010). Experimental investigation of three different solar air heaters: Energy and exergy analyses, 2953-2973.
8. Amit Kumar and Kishore, V.V.N., (1998). Utilization of solar pond technology in industry, Proc. National Solar Energy Convention of SESI, Dept. of Mechanical and Industrial Engg., University of Roorkee, Roorkee, 576-583.
9. Bansal, N.K., (1998). Emerging trends for energy efficiency in buildings, Invited lecture in National Solar Energy Convention of SESI, Deptt. of Mechanical and Industrial Engg., University of Roorkee, Roorkee, 11-20, Nov. 30 – Dec. 02.
10. Bevill, V.B. and Brandt, H., (1968). A solar energy collector for heating air, Solar Energy, 12, 19-29.
11. Biondi, P., Cicala, L. and Farina, G., (1988). Performance analysis of solar air heaters of conventional design, Solar Energy, 41, 101-107.
12. Bliss, R.W.,(1959). The derivation of several plate efficiency factor useful in design of flat plate solar heat collectors, Solar Energy, 3, 55-64.

13. Buchberg, H., Catton, I. And Edwards, D.K.,(1976). Natural convection in enclosed spaces A review of application to solar energy collection, *Trans. ASME, J. Heat Transfer,* **19**, 182-188.
14. Chiou, K.V. and Henderson, S.M., (1977). Performance of matrix solar collector for heating air, Trans. ASAE, 20(3), 558-561.
15. Cheema, L.S. and Mannan, D.K.,(1979). Performance of parallel flow packed bed air heaters, Proc. I.S.E.S., Silver Jubilee Congress, Atlanta, Georgia, 1, 259-263.
16. Chiou J.P., Wakil M.M. and Duffie J.A., (1965). A slit and expended aluminum foil matrix solar collector. *Solar Energy*, **9,** 73-80.
17. Choudhury, C., Anderson, S.L. and Rekstad, J., (1988). A solar air heater for low temperature applications, *Solar Energy,* **40**, 335-343.
18. Choudhury, C., Garg, H.P. and Prakash, J.,(1993). Design studies of packed-bed solar air heaters, Energy Convers., Mgmt. **34** (2), 125-138.
19. Choudhury, C. and Garg, H.P.,(1993). Performance of air hating collectors with packed air flow passages, *Solar Energy,* **50**, 205-221.
20. Cortes, A. and Piacentini, R., (1990). Improvement of efficiency of a bare solar collector by means of turbulence promoters, *Applied Energy*, **36**, 253-261.
21. Cortes, A. and Piacentini, R.,(2000). Improvement of Efficiency of a bare Solar Collector by means of turbulence promoter, Applied Energy, 253-261.
22. Cooper, P., Boyd, D., Thring, J.B. and Maw, R.G.,(1986). The highlands, Close group solar heating system (cost effective group solar heating), Report to the commission for the European Communities.
23. Demirel, Y. and Kunc, S.,(1987). Thermal performance study of a solar air heater with packed flow passage, *Energy Convers. Mgmt.*, **27** (3), 317-325.
24. Dhiman, Prashant., Thakur, N.S., Kumar, Anoop. Singh, Satyender., (2011). An analytical model to predict the thermal performance of a novel parallel flow packed bed solar air heater, Applied Energy,88, 2157-2167.
25. Esen, Hikmet.,(2007). Experimental energy and exergy analysis of a double-flow solar air heater having different obstacles on absorber plates, Building and Environment, 1046-1054.

26. Flores-Irigollen, A., Fernandez, J.L., Rubio-Cerda, E. ., Poujol, F.T.,(2004). Heat transfer dynamics in an inflatable-tunnel solar air heater, Renewable Energy,1367-1382.
27. Garg, H.P.,(1982). Treatise on Solar Energy, Vol. 1 : Fundamentals of Soar Energy, John Wiley, New York,
28. Gupta, M.K., Kaushik, S.C.,(2009). Performance evaluation of solar air heater for various artificial roughness geometries based on energy, effective and exergy efficiencies, Renewable Energy,465-476.
29. Hasatani, M., Itaya, Y. and Adachi, K.,(1985). Heat transfer and thermal storage characteristics of optically semi-transparent material packed bed solar air heater, A Compendium and Festchrift for Prof. A Ramachandran, ISHMT, Dept. of Mechanical Engg., I.I.T., Madras, India, 61-70.
30. Heggs, P.J.,(2000). Experimental techniques and correlations for heat exchanger surfaces : Packed beds, low Reynolds Number Flow Heat Exchangers edited by Kakac, S. Shah, R.K. and Bergeles, A.E.
31. Hottel, H.C. and Whillier, A.,(1955). Evaluation of flat plate collector performance, Trans. Conf. on the use of Solar Energy, 2 (1), 74-104, University of Arizona Press.
32. Hottel, H.C. and Woertz, B.B.,(1942). The performance of flat plate solar heat collectors, *Trans. A.S.M.E*, **64**, 91-104.
33. Jain, Dilip.,(2006). Modeling the performance of the reversed absorber with packed bed thermal storage natural convection solar crop dryer, Jurnol of Food Engineering, , 637-647.
34. Kakac, S., Shah, R.K. and Bergles, A.E.,(1983). Low Reynolds Number flow heat exchangers, Hemisphere Publishing Corporation, New York.
35. Klein, S.A.,(1975). Calculation of flat plate collector loss coefficients, *Solar Energy*, **17**, 79-80.
36. Kunii, D. and Smith, J.M.,(1960). Heat transfer characteristics of porous rocks, *A.I. Ch.E. Journal*, **6**, 71-80.
37. Liu, Ye-Di, Diaz, L.A. and Suryanarayana, N.V.,(1984). Heat transfer enhancement in air heating flat-plate solar collectors, *Trans. ASME, J. of Solar Energy Engg.*, **106**, 358-363.
38. Malhotra, A., Garg, H.P. and Palit, A.,(1981). Heat loss calculation of flat plate solar collectors, *The J. of Thermal Engineering*, **2**(2), 59-62.

39. Malhotra, A., Garg, H.P. and Rani, U.,(1980). Minimizing convective heat loses in flat plate solar collectors, *Solar Energy*, **25** (6), 521-526.
40. Mani, A., Methodologies for assessing solar energy potential, Proc. U.S.,(1985). India Symposium Workshop on Solar Energy Research and Application, Deptt., of Mechanical and Industrial Engg., University of Roorkee, Roorkee, 133-146.
41. Mishra, C.B. and Sharma, S.P.,(1981) Performance study of air-heated packed bed solar energy collector, *Int. J. Energy*, **6**, 153-157.
42. Mittal,M.K., Varun., Saini,R.P., Singal,S.K.,(2007). Effective efficiency of solar air heaters having different types of roughness elements on the absorber plate, Energy 32, 739-745.
43. Mullick, S.C. and Samadarshi, S.K.,(1988). An improved technique for computing the top loss factor of a flat plate collector with a single glazing, *J. of Solar Energy Engg*., **110**, 262-267,.
44. Paul, B., Saini, J.S.,(2004). Optimization of bed parameters for packed bed solar energy collection system, Renewable Energy,1863-1876.
45. Prasad, K. and Mullick, S.C.,(1985). Heat trnsfer characteristics of a solar air heater used for drying purposes, *Applied Energy*, **13**, 83-93.
46. Naphon Paisarn,(2005). Effect of porous media on the performance of the double-pass flat plate solar air heater, Heat and Mass Transfer., 140-150.
47. Naphon Paisarn,(2005). On the performance and entropy generation of the double-pass solar air heater with longitudinal fins, Renewable Energy,1345-1357.
48. Omojaro A.P., Aldabbagh, L.B.Y.,(2010). Experimental performance of single and double pass solar air heater with fins and steel wire mesh as absorber, Applied Energy, 3759-3765,.
49. Oozturk, H.H., Bascetincelik, A.,(2003). Energy and Exergy Efficiency of a Packed-bed Heat Storage Unit for Greenhouse Heating,Biosystem Engineering,231-245.
50. Ozgen, Filiz., Esen, Mehmet., Esen, Hikmet.,(2009). Experimental investigation of thermal performance of a double-flow solarair heater having aluminium cans, Renewable Energy, 2391-2398.

51. Pangavhane, D.R., Sawhney, R.L. and Sarsawadia, P.N.,(1998). Development of a multipurpose solar crop dryer, Proc. National Solar Energy convention of SESI, Deptt., of Mechanical and Industrial Engg., University of Roorkee, Roorkee, 315-322,
52. Prasad, R.K. and Saini, J.S.,(1993). Comparative performance study of packed bed solar air heaters, Emerging trends in Mech. Engg., Proc. Of 8th ISME Conference on Mech. Engg., I.I.T., Delhi.
53. Rady, Mohamed.,(2009). Thermal performance of packed bed thermal energy storage units using multiple granular phase change composites, Applied Energy, 2704-2720.
54. Reddy, T.A. and Gupta,(1980). C.L. Generating application design data for solar air heating systems, *Solar Energy*, **25**, 527-530.
55. Satcunanathan, S. and Deonarine, S.,(1973). A two pass solar air heater, *Solar Energy*, **15**, 41-49.
56. Sharma, S.P., Saini, J.S. and Varma,(1991). H.K., Thermal performance of packed bed solar air heaters, *Solar Energy*, **47**, 59-67.
57. Sharma, S.P., Saini, J.S. and Varma, H.K.,(1989). Performance of packed bed absorbers for solar air heaters, 10th National Heat and Mass Transfer Conference (India), 521-525, Srinagar.
58. Sharma, S.P., Investigations on thermal performance characteristics of solar air heaters with packed bed absorber, Ph.D. Thesis, Dept. of Mechanical and Industrial Engg., University of Roorkee, Roorkee, India, 1990.
59. Shoemaker, M.J., Notes on solar collector with unique air permeable media, *Solar Energy*, **5**, 138-141, 1961.
60. Singh, P., Cheap packed bed absorbers for solar air heaters, Proc. Int. Solar Energy Society Cong., Vol. II, New Delhi, 900-904, 1978.
61. Sodha, M.S., Bansal, N.K., Singh, D. and Bharadwaj, S.S.,(1982). Performance of a matrix air heater, *J. Energy*, **6** (5), 334-339.
62. Togrul, Inci Turk, Pehlivan, Dursun.,(2005). Effect of packing in the airflow passage on the performance of a solar air-heater with conical concentrator, Applied Thermal Energy, 1349-1362.

63. Varshney L. and Saini J.S. (1998). Heat transfer and friction factor correlations for rectangular solar air heater duct packed with wire mesh screen matrices. *Solar Energy*, 62 (4) : 255-262.
64. Wakao, N., Kaguei, S. and Funazakri, T., Effect of fluid dispersion coefficient on particle to fluid heat transfer coefficient in packed beds, *Chem. Engg. Sci.*, **34**, 325-336, 1979.
65. Wijeysundara, N.E., Ah, L.L. and Tjioe, L.E.,(1982). Thermal performance study of two pass solar air heaters, *Solar Energy*, **28** (5), 363-370.
66. Xu, J., Tian, J., Lu, T.J., Hodson, H.P.,(1982). On the thermal performance of wire-screen meshes as heat exchanger material, Heat and Mass Transfer, 1141-1154.
67. Yagi, S., Kunii, D.,(1957). Studies on effective thermal conductivities in packed beds, *A.I. Ch. E. Journal* , **3** (3), 373-381.

Appendix

```
//Simple Solar Air Heater

#include<iostream.h>

#include<conio.h>

#include<math.h>

//ALL UNITS ARE SI

float L=4, W=1;                 //length, Width

float s=.02;                    //Plate to Cover Spacing

float Ep=.1, Ec=.88;            //Emsivity of Plate, Emsivity of Cover

float at=.82;                   //Transmisisvity absorptivity product

float I=900;                    //Radiation incident on plate

float Ti=333;                   //Inlet air temperature

float To,Tmp,Tmf;               //airOutlet ,mean plate &fluid tem

float Tp=343, Tf=343, Ta=283, T=308;

//Mean Temperature of Plate is assumed, Fluid, Ambient air Temperature, Mean
      //Temperaturebetween plate and cover

float hw;                       //convection coefficent of Wind

float Ut,UL;                    //Top&Overall heat transfer coefficient

float den,V, mu=.0000204,m=.056, Cp=1009;  //Density & VelocityDynamic
      //viscocity,mass /flow rate
```

```
float Ac=4,Af=.01;              //area of cross-section & area of flow

float Dh=2*s, F1, F2, FR;       //Hydraulic diameter,s is spacing, Collector efficinecy //factor,
      Collector flow factor, Collector heat removal factor

void main()

{float Tc=308;                  //Mean Temperature ofCover is assumed

float v=1.96E-5;                //kinematic viscosity

float Sg=5.67E-8;               //Stefan boltzman Constant

float hrpc,hrca,hcpc;           //r-Radiahrcation,c-Convection

float h,k=.0293;                //convective &conduction heat transfer coefficient of air

float Ra,Pr=.7, Nu=3.73;        //Rayleigh numer,prandel no., nusselt no.

hrpc=(Sg*pow(Tp,2)+pow(Tc,2)*(Tp+Tc))/((1/Ep)+(1/Ec)-1);

hrca=Sg*Ec*(Tc*Tc*Tc+Ta*Ta)*(Tc+Ta);

Tc=Tp-(Ut*(Tp-Ta)/(hcpc+hrpc));

Ra=9.81*(Tp-Tc)*s*s*s*Pr/(T*v*v);

h=Nu*k/Dh;

Ut=1/((1/(hcpc+hrpc))+(1/(hw+hrca)));

UL=1+Ut;

float hr=(4*Sg*Tf*Tf*Tf)/((1/Ep)+(1/Ec)-1);

float Re=m*Dh/Af*mu;

Nu=.0158*pow(Re,0.8);
```

```
F1=(1+(UL/(h+(1/((1/h)+(1/hr))))));

float con=m*Cp/(Ac*UL*F1);

float con1=-1/con;

F2=con*(1-exp(con1));

FR=F1*F2;

float Qu=Ac*FR*(I*at-UL*(Ti-Ta));//Useful gain

To=Ti+Qu/(m*Cp);

Tmp=Ti+Qu*(1-FR)/FR*UL*Ac;

Tmf=Ti+Qu*(1-F2)/FR*UL*Ac;

float err1=fabs(Tmp-Tp);

float err2=fabs(Tmf-Tf);

if ((err1>.01)&(err2>.02))

{Tp=Tmp, Tf=Tmf;}

else

{float neff=Qu/(Ac*I);

float tr=(To-Ti, ro=1.2, v=m/(ro*Af)), fs=0.085/pow(Re,0.25);

float dp=(4*fs*L*ro*v*v)/(2*Dh, Q=m/ro);

float Pm=Q*dp, c=0.12;

float qm=Pm/c;
```

```
float Neff=(Qu-qm)/(I*Ac);
cout<<"Net thermal gain Qu                    ="<<  "<<Qu<<"      "<<"W"<<endl;
cout<<"Pumping power Pm/c                     ="<<  "<<qm<<"      "<<"W"<<endl;
cout<<"Effective efficiency                   ="<<  "<<Neff<<endl;
cout<<"Thermal efficiency                     ="<<  "<<neff<<endl;
cout<<"Renold Number Re                             ="<<  "<<Re<<endl;
cout<<"Temp.Rise parameter (To-Ti)/I="<<"         "<<tr<<endl;}}
//PacedBed Splar air Heater
#include<math.h>
#include<iostream.h>
#include<conio.h>
void main()
{       double dw,pt,n,m,ti,ta,I,P,b;
        double a[60][160];
        double G[60],x[60],H[10];
        int i,j,k,l;
        double L   = 2.39;                  //Length of heater
        double W   = 0.41;
        double Ac  = L*W;                   //Cross-sectional area or heat transfer area
```

```
double D   = .025;                  //Optical depth of channel

double Cp  = 1006;

double Sig = .0000000567;           //Steafen boltzman constant

double PI  = 3.14159;

double a1  = (PI*dw*dw*pt*n)/2;

double b1  = pt*pt*D;

double Af  = D*W;                   //frontal area of Colector bed


double A   = 4*Af*L*(1-P)/dw;       //Total heat transfer area

double av  = A/(Ac*D);              //Heat transfer area per unit voluem of
matrix

double Go  = m/(Af*P);              //Mass velocity of air

double De  = 6/av;

double ab  = 0.12;

double Ket = ab*De*Cp*Go;

double Kp  = 62.764;                //Thermal conductivity of matrix

double Tb  = ti+273+20;             //Mean bed temperature in Kelvin

double tb  = Tb/100;

double p   = P/(2*(1-P));

double e   =  0.8;                  //Emissivity of wire mesh screen
```

```
double e1  = (1-e)/e;

double c1  = 1+p*e1;

double hrv = (0.1953*pow(tb,3))/c1;

double e2  = e/(2-e);

double hrs = 0.1952*e2*pow(tb,3);

double p1  = pow(P,1.3);

double d1  = (hrv*De*p1)/(1-p1);

double f1  = 1/(Kp+d1);

double phi = 0.12;                                  //Ratio of effective thickness of fluid film to

double Kg  = 0.0267, g1  = 1/((Kg/phi)+hrs*De);     //Thermal conductivity of air

  double h1  = 4*De*Kp*p1*hrv;

double j1  = Kp+d1+(Kg/phi)+hrs*De;

double n1  = 1.0;                                   //Refrective index of mesh material

double m1  = (16*n1*n1*Sig*pow(Tb,3))/(3*b);

double q1  = (1+p1)/(f1+g1);

double Keo = q1+(h1/j1)+m1;

double Ke  = Ket+Keo;

//Calculation for top loss cefficient

int N      = 2;                                     //No. of glass covers
```

```
double hw  = 10.0, B   = 20.0;            //Wind heat transfer coefficient, collector tilt

double ep  = 0.8, eg  = 0.88;             //Emittance of plate, Emittance of Glass cover

double Ta  = ta+273;

double F   = (1+0.89*hw-0.1166*hw*ep)*(1+0.07866*N);

double E   = 0.43*(1-100/Tb);

double C   = 520*(1-0.000051*B*B);

double a2  = (Tb-Ta)/(N+F);

double b2  = (C*pow(a2,E))/Tb;

double c2  = (N/b2)+1/hw;

double d2  = Sig*(Tb+Ta)*Tb*Tb*Ta*Ta;

double e3  = (1/(ep+0.00591*N*hw))+((2*N+F-1+0.133*ep)/eg)-N;

double Ut  = (1/c2)+(d2/e3);

//calculation for non dimensional parameters

double Uto = Ut/(Ke*b);

double tao = ta/ti;

double u   = .00001865;                   //viscocity of air

double Pr  =(u*Cp)/Kg;                    //Prandtl No.

double f2  =pow(Pr,2/3);

double rh  = P*dw/(4*(1-P));
```

```
double Rep = (4*rh*Go)/u;

double g2  =  pt/(n*P*dw);

double h2  = pow(g2,2.104);

double Jh  = (0.647*h2)/pow(Rep,0.55);          //Colburn j factor

double hc  =  (Jh*Go*Cp)/f2;

double hv  =  hc*av;

double hvo = (2*hv*L)/(P*Go*Cp);

double hvoo= (2*hv)/(Ke*b*b);

double rc  = 0.0434;                            //reflectivity of glass cover

double Teff= 0.72;                              //efective transmittance

double To  = b*D;

double l2  = exp(To);

double m2  = 1-(rc*(1-ep))/(l2*l2);

double R1  =(I*Teff)/m2;

double R2  = (R1-I*Teff)/(rc/l2);

double Ro1 = R1/(Ke*b*ti);

double Ro2 = R2/(Ke*b*ti);

//calculate constants

int M1 = 5;                 //No.of nodes in Y direction
```

```
int N1 = 5;                    //No.of nodes in X direction

double h =To/(M1-1);

double K = L/(N1-1);

double C1 = 1/(1+h*Uto);

double C2 = h*Uto*tao*C1;

double C3 = 1/(1+hvoo*h*h);

double C4 = hvoo*h*h*C3;

double C5 = 1/(1+K*hvo);

double C6 = K*hvo*C5; j=5;

double T =(j-1)*h;

double Qro =(Ro1/exp(T))-Ro2/exp(To-T);

double C7= h*Qro;

for(j=2;j<=4;j++)

{ T=(j-1)*h;

   H[j] =(C3*h*h)*(Ro1/exp(T))-(Ro2/exp(To-T)); }

//read matrix

for(i=1;i<=50;i++)

for(j=1;j<=50;j++)

 a[i][j]=0;
```

```
for(i=1;i<=50;i++)
{ j=i;
a[i][j]=1;}
for(i=1;i<=41;i=i+10)
{ j=i+2;
a[i][j]=-C1;        }
i=1;
for(l=1;l<=5;l++)
{ for(k=1;k<=3;k++)
{ i=i+2;
j=i+2;
a[i][j]=-C3; }
i=i+4; }
i=1;
for(l=1;l<=5;l++)
{  for(k=1;k<=3;k++)
{ i=i+2;
j=i-2;
a[i][j]=-C3;}
```

```
i=i+4;     }
i=1;
for(l=1;l<=5;l++)
{ for(k=1;k<=3;k++)
{ i=i+2;
j=i+1;
a[i][j]=-C4; }
i=i+4;}
for(i=12;i<=50;i=i+2)
{ j=i-10;
a[i][j]=-C5; }
for(i=12;i<=50;i=i+2)
{ j=i-1;
a[i][j]=-C6;}
for(i=9;i<=49;i=i+10)
{ j=i-2;
a[i][j]=-1; }
for(i=1;i<=41;i=i+10)
G[i]=C2;
```

```
for(i=2;i<=10;i=i+2)

G[i]=1;

for(i=3;i<=43;i=i+10)

G[i]=H[2];

for(i=5;i<=45;i=i+10)

G[i]=H[3];

for(i=7;i<=47;i=i+10)

G[i]=H[4];

for(i=9;i<=49;i=i+10)

G[i]=C7;

for(i=12;i<=50;i=i+2)

G[i]=0;

//Gauss elimination

for(k=1;k<=49;k++)

{ double pivot=a[k][k];

for(i=k+1;i<=50;i++)

{ double factor =a[i][k]/pivot;

for(j=1;j<=50;j++)

{ a[i][j]=a[i][j]-factor*a[k][j]; }
```

```
   G[i]=G[i]-factor*G[k]; }}

   x[50]=G[50]/a[50][50];

   for(k=49;k>=1;k--)

   { double sum=0.000;

   for(j=k+1;j<=50;j++)

   {sum=sum+a[k][j]*x[j]; }

   x[k]=(G[k]-sum)/a[k][k]; }

//Calculation forn effective efficyency

double SUM =0.00;

for(i=42;i<=50;i+2)

SUM=SUM+x[i];

double to = (ti*SUM)/5;

double qu = m*Cp*(to-ti);

double tx = (to-ti)/I;

double a4 = pt/(n*P*dw);

double fp = 2.484*pow(a4,0.699)/pow(Rep,0.44);

double ro = 1.2;                          //air density

double v  = m/(ro*Af*P);                  //Velocity of air

double dP = ro*v*v*L*fp/(2*rh), Q  = m/ro;
```

```
double Pm = Q*dP, c  = 0.18;

double qm = Pm/c;

double THeff = qu/(i*Ac);

double Eeff = (qu-qm)/(I*Ac);

cout<<"Thermal energy gain Qu                =="<<qu<<"     "<<"W"<<endl;

cout<<"Pumping power Pm/c                    =="<<qm<<"     "<<"W"<<endl;

cout<<"Efective efficiency                   =="<<Eeff<<endl;

cout<<"Thermal Efficiency                    =="<<THeff<<endl;

cout<<"Reynold Number Re                     =="<<Rep<<endl;

cout<<"Temperature Rise Parameter (To-Ti)/I=="<<tx<<endl;}
```